DESIGN OF ENVELOPE TRACKING POWER AMPLIFIER FOR LTE APPLICATIONS

BY

MOHAMED OSMAN HUSSEIN KHALIFA

A Thesis Presented to the

DEANSHIP OF GRADUATE STUDIES

KING FAHD UNIVERSITY OF PETROLEUM & MINERALS

DHAHRAN, SAUDI ARABIA

In Partial Fulfillment of the
Requirements for the Degree of

MASTER OF SCIENCE

In

ELECTRICAL ENGINEERING

MAY 2015

KING FAHD UNIVERSITY OF PETROLEUM & MINERALS

DHAHRAN- 31261, SAUDI ARABIA

DEANSHIP OF GRADUATE STUDIES

This thesis, written by **MOHAMED OSMAN HUSSEIN KHALIFA** under the direction of his thesis advisor and approved by his thesis committee, has been presented and accepted by the Dean of Graduate Studies, in partial fulfillment of the requirements for the degree of **MASTER OF SCIENCE IN ELECTRICAL ENGINEERING.**

Dr. Oualid Hammi
(Advisor)

Prof. Azzedine Zerguine
(Member)

Dr. Khurram K. Qureshi
(Member)

Dr. Ali Ahmad Al-Shaikhi
Department Chairman

Dr. Salam A. Zummo
Dean of Graduate Studies

17/5/15

Date

DESIGN OF ENVELOPE TRACKING POWER AMPLIFIER FOR LTE APPLICATIONS

MOHAMED OSMAN HUSSEIN KHALIFA

ELECTRICAL ENGINEERING

MAY 2015

KING FAHD UNIVERSITY OF PETROLEUM & MINERALS

DHAHRAN- 31261, SAUDI ARABIA

DEANSHIP OF GRADUATE STUDIES

This thesis, written by **MOHAMED OSMAN HUSSEIN KHALIFA** under the direction of his thesis advisor and approved by his thesis committee, has been presented and accepted by the Dean of Graduate Studies, in partial fulfillment of the requirements for the degree of **MASTER OF SCIENCE IN ELECTRICAL ENGINEERING.**

_____

Dr. Oualid Hammi
(Advisor)

_____

Dr. Ali Ahmad Al-Shaikhi
Department Chairman

_____

Prof. Azzedine Zerguine
(Member)

_____

Dr. Salam A. Zummo
Dean of Graduate Studies

_____

Dr. Khurram K. Qureshi
(Member)

_____

Date

-

Dedicated to my

Parents, siblings and their sacrifices

And to my small family

Anan Ibrahim

ACKNOWLEDGMENT

All praise, glory and gratitude is for Allah, the most beneficent, the most merciful.

I thank my advisor Dr. Oualid Hammi for introducing me to the field of power amplifiers design and linearization to which I was bliss-fully unaware and also rekindling my interest in Microwave and electronics in general. Working with him was very enlightening experience and i really consider him one of the few people who have shaped my outlook and attitude towards research and life in general. I also thank him for all the support, encouragement, suggestions and bearing with me with his infinite reserves of patience.

I would like to thank my committee member Prof. Azzedine Zerguine and Dr. Khurram K. Qureshi for their valuable suggestions, positive feedback and investing time to be part of my thesis committee.

I would like also to send my sincere thanks to my friends, mentors, and advisors at University of Calgary-iRadio Lab for helping, guiding, and advising me through my stay there. Special thanks to Prof. Fadhel Gannouchi for giving me the chance to be a visiting student at iRadio Lab. Many thanks also to Mr. Andrew Kwan for training, guiding, and introducing me to the facilities and equipments in iRadio Lab.

I'm grateful to my friend Abubaker Abdelhafiz who always helped me and supported me through my journey towards my Master degree.

I would also like to thank KFUPM for providing world class facilities and their support throughout my stay here in Saudi Arabia.

TABLE OF CONTENTS

LIST OF TABLES

LIST OF FIGURES

LIST OF ABBREVIATIONS

ACLR	:	Adjacent Channel Leakage Ratio
ACPR	:	Adjacent Channel Power Ratio
CCDF	:	Complementary Cumulative Distribution Function
CS	:	Compressed Sampling
DAC	:	Digital to Analog Converter
DPD	:	Digital Predistortion
DUT	:	Device Under Test
ED	:	Envelope Dependent
EE&R	:	Envelope Elimination and Restoration
EMP	:	Envelope Memory Polynomial
ET	:	Envelope Tracking
ETPA	:	Envelope Tracking Power Amplifier
ETSI	:	European Telecommunications Standard Institute
FM	:	Frequency Modulated
FPGA	:	Field Programmable Gate Array
GaN	:	Gallium Nitride
GMP	:	Generalized Memory Polynomial

GMSK	:	Gaussian Minimum Shift Keying
IMD3	:	Third order Intermodulation Distortion
LS	:	Least Squares
LTE	:	Long Term Evolution
LUT	:	Look-Up Table
LUT-SISO	:	Look-Up Table Single-Input-Single-Output
LUT-MISO	:	Look-Up Table Multi-Input-Single-Output
MISO	:	Multi-Input-Single-Output
MP	:	Memory Polynomial
NMSE	:	Normalized Mean Squared Error
OFDM	:	Orthogonal Frequency Division Multiplexing
PA	:	Power Amplifier
PAE	:	Power Added Efficiency
PAPR	:	Peak to Average Power Ratio
PDF	:	Probability Density Function
PLUME	:	Parallel-LUT-MP-EMP
QAM	:	Quadrature Amplitude Modulation

RF	:	Radio Frequency
SDD	:	Symbolically-Defined Device
TNTB	:	Twin Nonlinear Two-Box
UMTS	:	Universal Mobile Telecommunication System
VSA	:	Vector Signal Analyzer
VSG	:	Vector Signal Generator
WCDMA	:	Code Division Multiple Access
WiMAX	:	Worldwide Interoperability for Microwave Access

ABSTRACT

Full Name : Mohamed Osman Hussein Khalifa

Thesis Title : Design of Envelope Tracking Power Amplifiers for LTE Applications

Major Field : Electrical Engineering

Date of Degree : May, 2015

A conventional RF power amplifier designed with a fixed supply voltage operates most efficiently when it is in compression, and becomes less efficient as signal peak to average power ratio increases because the amplifier spends more time operating below peak power and, therefore, spends more time operating below its maximum efficiency. However, the use of envelope tracking technique can dramatically increase the efficiency of radio frequency transmitters. In this thesis, a design approach suitable for power amplifiers intended for envelope tracking systems is proposed. The selection of the load reflection coefficient is made based on the use of amplifier in the envelope tracking configuration, and thus takes into account the nature of the signal to be used and the shaping function to be applied. A comparison between conventional design approach for the choice of the reflection coefficient and the proposed method is reported.

Moreover, strong nonlinearities of envelope tracking power amplifiers are addressed. These can lead to violations of the spectral emission mask if not countered with digital predistortion (DPD). In this thesis Volterra-series with compressed sampling and two-box dual input models have been proposed for modeling and digitally predistorting ETPA respectively. The two models have proved their accurate modeling and linearization performance through measurement results.

ملخص الرسالة

الاسم الكامل: محمد عثمان حسين خليفة

عنوان الرسالة: تصميم مضخمات القدرة متابعة الغلاف لتطبيقات التطور طويل الأمد

التخصص: الهندسة الكهربائية

تاريخ الدرجة العلمية: مايو، 2015

مضخمات القدرة التقليدية المستخدمة في الترددات الرادوية تستعمل مصادر فولتية ثابتة، و عادة ماتكون أكثر كفاءة عندما تعمل في طور الانضغاط، بينما تقل كفاءتها عندما تتعاظم نسبة ذروة الإشارة إلى متوسطها وذلك لأن المضخم يقضي وقتا أطول وهو يعمل بقدرة أقل من قدرة الذروة؛ ونتيجة لذلك فإن المضخم يعمل بكفاءة أقل من كفاءته العليا. لحل هذه المشكلة فإن مضخمات القدرة متابعة الغلاف تستعمل لزيادة كفاءة مرسلات الترددات الرادوية. في هذه الأطروحة، اقترحت طريقة تصميم مناسبة لتصميم مضخمات القدرة التي ينوى استعمالها مع انظمة متابعة الغلاف حيث أن اختيار معامل انعكاس الحمل يتم بناءا على خلفية أن المضخم سوف يستعمل في منظومة متابعة الغلاف؛ لذلك يأخذ في الاعتبار طبيعة الإشارة المستعملة و دالة التشكيل المنفذة. كما تم عقد مقارنة بين الطريقة التقليدية والطريقة المقترحة لاختيار معامل انكسار الحمل.

في هذه الأطروحة تم تناول اللاخطية الملازمة لمضخمات القدرة متابعة الغلاف التي من شأنها أن تؤدي إلى اختراقات في قناع الانباعاثات الطيفية مالم تواجه بالتشويه الرقمي الاستباقي (DPD). كما تم اقتراح سلسلة فولتيرا مع أخذ العينات المضغوط لنمذجة مضخم القدرة متابع الغلاف بينما اقترح نموذج الصندوقين ذو المدخلين لغرض التشويه الرقمي الاستباقي للمضخم. كلا النموذجين أثبتا دقتهم في نمذجة و تقويم مضخمات القدرة متابعة الغلاف عن طريق نتائج القياسات العملية.

CHAPTER 1

INTRODUCTION

In the last decade, scientists, researchers, and engineers have given focus to energy saving techniques in order to reduce the emission of carbon dioxide (CO2) and consequently alleviating the problem of global warming.

According to European Telecommunications Standard Institute (ETSI) report [1], radio units account for over 90% of the energy consumed by wireless communication units. Moreover, 50% to 80% of the radio unit energy is consumed by the power amplifier (PA). Besides the consumption of the radio unit, around 10% to 25% of the energy is used for air conditioning, 5% to 15% for signal processing and the rest to the power supply units. Furthermore, energy consumed by air conditioning could be reduced by improving the efficiency of the power amplifiers. Therefore, improving the efficiency of the PA reduces the power consumption of radio unit since most of the consumption is attributed to it.

Competing with the demand for high efficiency, linearity has risen in importance in the last decade. In previous generations, constant envelope signals such as Gaussian Minimum Shift Keying (GMSK) signals and Frequency Modulated (FM) signals were used to avoid linearity constraints since these constant amplitude signals are not affected by the nonlinearity of the PA. However, there is an increasing demand for spectral efficiency in wireless technology. This is driven by the consumer need for high data rate

and more real time media content. This demand has led to the introduction of many wireless communication standards (Universal Mobile Telecommunication System (UMTS), Long Term Evolution (LTE), and Worldwide Interoperability for Microwave Access (WiMAX) standards) with increasingly complex modulation schemes (such as Quadrature Amplitude Modulation (QAM)) and access technologies (Wideband Code Division Multiple Access (WCDMA) and Orthogonal Frequency Division Multiplexing (OFDM)), which use both phase and amplitude modulation. These modulation schemes are characterized by high peak to average power ratio (PAPR) signals. Hence, modern PAs need to be extremely linear over a large power range.

1.1 RF Front-end for Communication Systems

Usually, PAs are biased in deep linear classes of operation (class A, AB) and they are operated in the back-off region in order to meet linearity requirements for high PAPR signals. Unfortunately, PAs biased in these classes have very low efficiency when they are backed-off. Conversely, more efficient classes of PAs are extremely nonlinear and thus not a suitable alternative. These conflicting parameters (linearity and efficiency) have brought great attention to the PA; since the power amplifier is the main source of distortion and the most power hungry device in the Radio Frequency (RF) front end.

Envelope tracking PA (ETPA) is one of the most promising structures that could be used for future wireless communication infrastructure. Unlike regular constant drain bias PAs, ET allows the power amplifier drain bias to track the magnitude of the input signal envelope keeping the amount of wasted DC power at the drain bias to minimum, which greatly improves the PA efficiency.

Linearity could be improved by using linearization techniques such as feedforward and baseband digital predistortion (DPD). However, feedforward linearization techniques need analog delay elements for phase matching which might be very challenging in wideband applications. DPD is an ideal complement to the ETPA; it allows linearization flexibility and bandwidth while at the same time, keeping the high efficiency of the ETPA.

1.2 Constant and Modulated Supply Power Amplifiers

An amplifier is a device designed to increase the input signal power levels. The basic principle of operation is that it takes energy from the power supply and controls the output signal to match the shape of the input signal but with higher amplitude. Therefore, fundamentally an amplifier modulates the power supply output. Different types of amplifiers are available specially designed for different requirements and applications.

A power amplifier is usually the final amplification stage in a system, designed to give the required output power. From communications systems perspective, power amplifiers are mainly present in transmitters and are specifically designed to raise the input signal power level before passing it to antenna. Having this power boost is fundamental for the desired signal to noise ratio to be achieved on the receiver end, without which it will be difficult to detect the received signal.

1.2.1 Constant Supply Power Amplifiers

It is necessary for the constant supply power amplifier to have as high efficiency as possible while at the same time maintaining linearity, i.e., adding as little distortion to the

signal as possible. High power efficiency is of prime importance in small and mobile transmitters, since these devices are usually driven by battery. It is also important for base stations as it affects their deployment and operating costs as well as their carbon foot print. Unfortunately, from circuit design point of view, if the power efficiency is increased the device is driven more and more into the nonlinear region thus increasing the amount of distortion.

Efficiency and linearity considerations lead to various classes of power amplifiers such as class A, class B, class AB, class C, etc. Each one of them has its own tradeoff between linearity and efficiency depending on how the PA's transistor is biased. Figure 1.1 and Figure 1.2 illustrate this tradeoff. As it can be noticed, interesting improvements in efficiency is achieved when moving from linear class of operation such as class A to nonlinear classes of operations such as class AB and class B and that is done by reducing the conduction angle. Clearly, improving the efficiency leads to stronger nonlinearity since it comes at the cost of increasing output harmonic components [2].

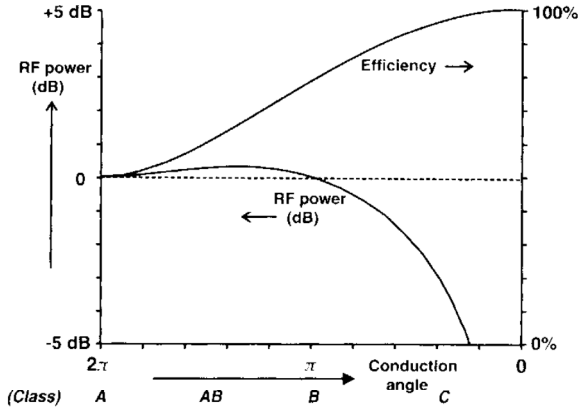

Figure 1.1: PA efficiency VS PA's class of operation [2]

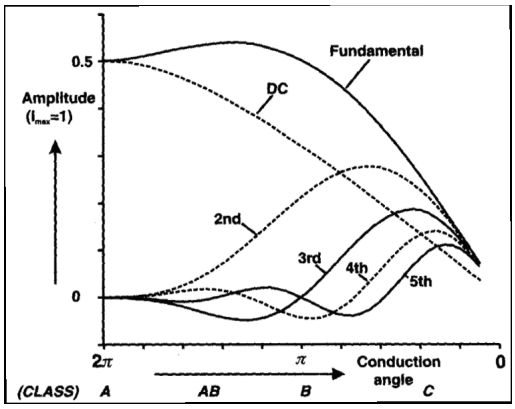

Figure 1.2: PA Nonlinearity VS PA's class of operation [2]

Thus, methods for improving the PA efficiency in the back-off region without compromising the linearity are needed. This can be done by using an efficient and nonlinear PA along with a linearization technique. Recent base stations have adopted digitally predistorted Doherty PA [3] as the main power efficient solution. However, the efficiency figures obtained by Doherty PA can be overcome through the use of other promising efficiency enhancement techniques such as polar transmitters, envelope elimination and restoration (EE&R), or envelope tracking. Among these, ET is the catchiest one regarding practical implementation because it can be applied by simply replacing the static supply by a dynamic one in conventional transmitters based on linear RF amplification topologies. Moreover, ET shows a significant improvement in the average power added efficiency (PAE), this result is well known in the literature [4].

1.2.2 Envelope Tracking Power Amplifiers

High PAPR is a basic and unavoidable feature in modern modulated signals. For the signal not to be distorted when its envelope excursion is near its peak, constant drain PAs are usually operated in deep back-off. Since the amplifier is efficient only when operating in compression but spends more time operating far below its maximum efficiency, poor

average efficiency is obtained. Figure 1.3 shows a conventional power amplifier system operating with a constant DC supply.

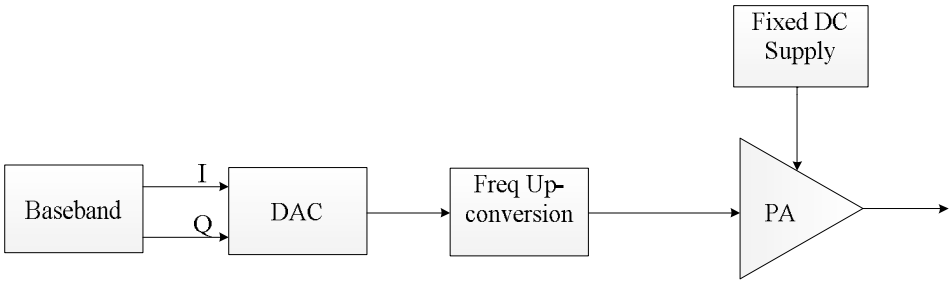

Figure 1.3: Conventional RF power amplifier.

ET is a method to solve this low efficiency issue; since it allows the drain bias of the PA to track the magnitude of the envelope of the input signal. Thus, whenever the input signal is low the drain bias proportionally decreases so that the PA always operates close to its optimum efficiency point [5] for low and high input power levels. Figure 1.4 shows a block diagram for ETPA.

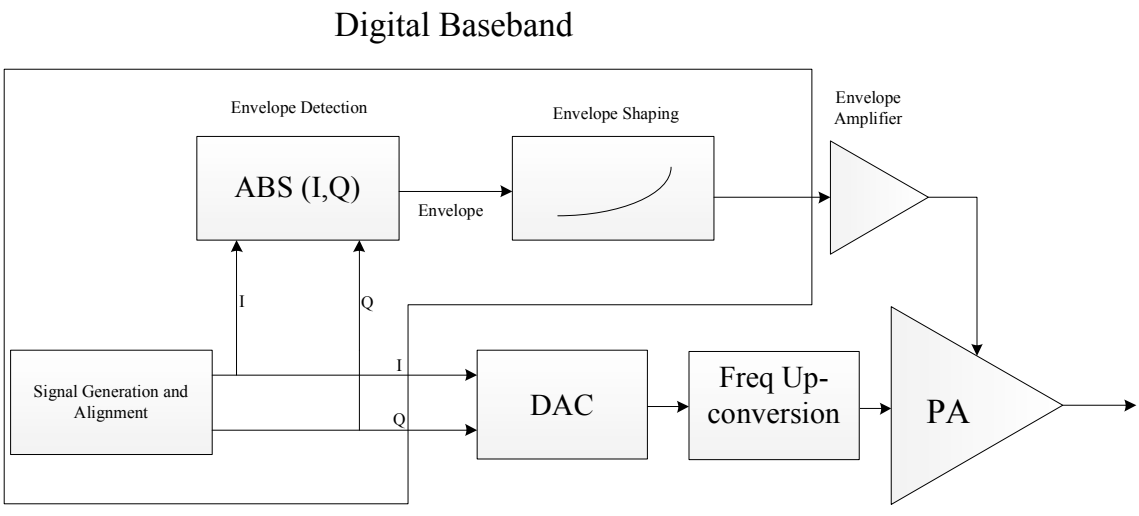

Figure 1.4: ETPA block diagram.

ET systems improve the efficiency but often result in poor linearity performance since the bias of the amplifier is varying. Both, the linearity and the efficiency performance of the ET power amplification system depend on several factors such as the efficiency of the supply modulator, the efficiency of the power amplifier, and the mapping function (also called envelope shaping function) used to map the signal's envelope into a variable drain supply voltage. In ETPA, the fundamental characteristics of the PA output (efficiency, power, gain, and phase) are functions of two control inputs, namely the RF input signal and the drain bias voltage and this relation could be represented as 3-D surface as depicted in Figure 1.5.

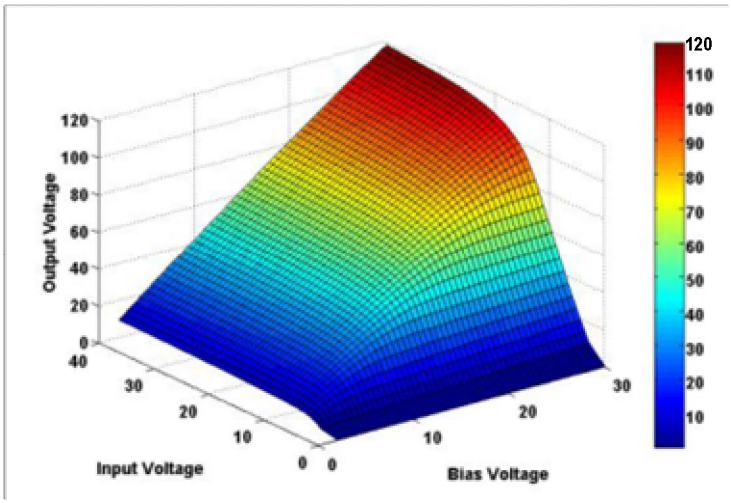

Figure 1.5: 3-D relationship between input, drain Bias, and output voltages [6].

Three regions of operation could be differentiated when dealing with ETPA. The first one is called the compressed region and it can be noticed when the instantaneous RF input power is high. In this region, the PA operates with high efficiency in compression and the drain bias voltage primarily determines the PA's output characteristics. The second region, called the linear region, arises when the instantaneous RF input power is low. In

this region, the drain bias voltage remains substantially constant and the PA's output characteristics are mainly determined by the instantaneous RF input power. Between these two regions, there is a region called the transition region; in which the PA's output characteristics are under the influence of both the drain bias voltage and the instantaneous RF input signal as can be seen in Figure 1.6.

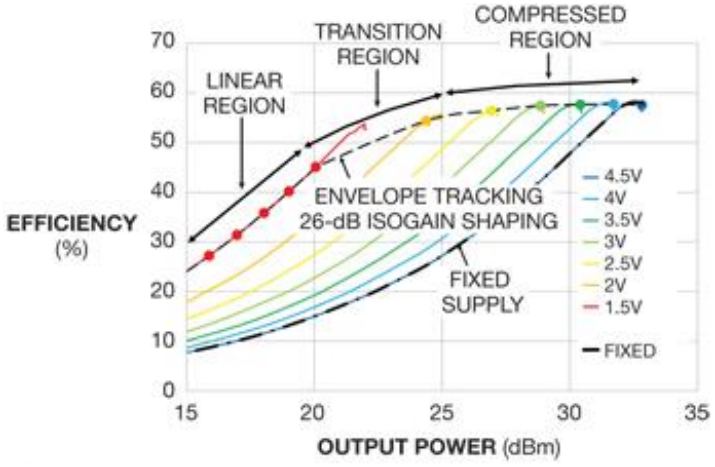

Figure 1.6: ETPA operation regions

Having this high efficiency of the ETPA, linearization techniques need to be used to meet the linearity requirements set by the regulatory bodies.

1.3 Behavioral Modeling and Digital Predistortion

Due to the degradation in linearity caused by the use of the ETPA, linearization techniques should be used to enhance the linearity of the ETPA in order to meet modern communication standards linearity requirements. Furthermore, linearization indirectly enhances the PA efficiency; since the linearized PA usually operates in compressed

region allowing us to operate the PA near its peak efficiency, despite the high nonlinearity in this region. In the literature, there are three most well established linearization methods: feedback, feedforward, and predistortion.

Feedforward linearization technique provides extremely linear characteristics as proposed in [7]. This technique however consists of complex control circuits and an auxiliary error power amplifier which increase the cost and degrade the efficiency. The feedback linearization technique proposed in [8] has the drawbacks of bandwidth limitation and instability. Among all the linearisation techniques, the most extensively used technique in modern wireless communication infrastructure is digital predistortion (DPD) for its high accuracy, flexibility and efficient operation [9]–[12].

Behavioral modeling and digital predistortion are two important techniques that are used in order to solve the nonlinearity problem that is exhibited by the base station power amplifiers. The idea is to have a digital predistorter, which typically has complementary characteristics of the PA, connected before the PA so that the two systems in cascade have a linear operation. This technique employs a black-box based approach. As shown in Figure 1.7, behavioral modeling identifies a mathematical formulation relating the input and output signals of the amplifier. Having information about the radio frequency circuitry of the PA is not required. Moreover, behavioral modeling provides a computationally efficient way to relate the input and output signals without performing any physical analysis of the system and it is thus a valuable process for assessment of the transmitter performance and design of the digital predistorter [13]. It is important to accurately obtain the device under test (DUT) input and output signals and the

mathematical formulation should be able to describe all the important interactions that occur between these signals. This requires some apriori knowledge of the DUT.

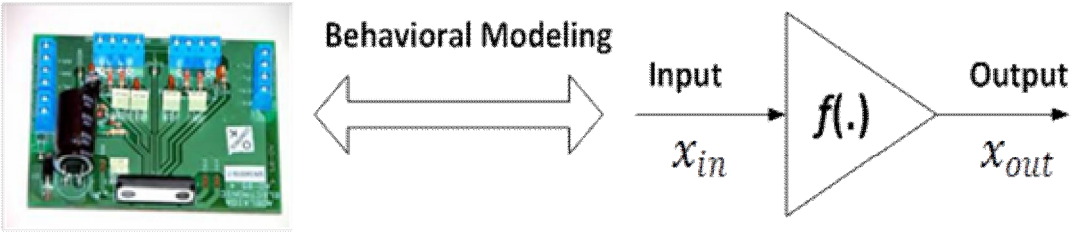

Figure 1.7: Black box behavioral modeling concept [13].

1.4 Nonlinear Distortion Metrics

Due to the modulation of the drain bias, the linearity of the ETPA is degraded compared with that of the constant drain PA. This degraded linearity could be observed in many ways; the one tone and two-tone tests are the most common tests used to characterize the nonlinear behavior of the PA. However, these two tests are simple and ideal for PA design debugging, thus the PA should be driven by a modulated signal so that its nonlinear behavior is fully characterized.

When the DUT is driven by modulated signals, two metrics could be used to characterize its nonlinear distortion. The first metric is the ACPR (analogous to the IMD3 in the two-tone test) and it is defined as the power ratio of the power in the transmit frequency channel to the power in the adjacent frequency channel. The ACPR is helpful in understanding the DUT nonlinear behavior and how it can interfere with the adjacent channels. Figure 1.8 shows the input and output spectra of a PA and it clearly illustrate the ACPR concept.

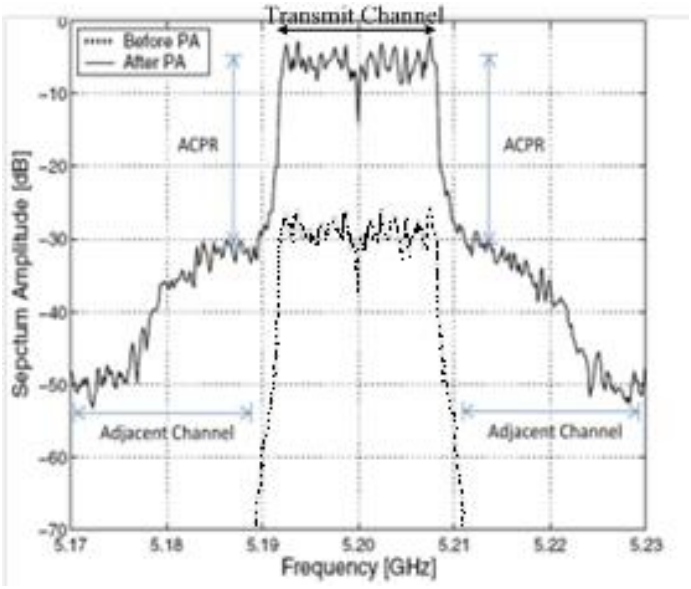

Figure 1.8: ACPR illustration in PA input and output spectrum.

Since the ACPR does not provide any information about how the transmitted signal gets distorted within the transmission channel, another metric that is the normalized mean squared error (NMSE) is mainly used to provide this information. The normalized mean squared error (NMSE) is given by

$$NMSE = \frac{\sum_{n=1}^{N} \left| y_{meas}(n) - y_{model}(n) \right|^2}{\sum_{n=1}^{N} \left| y_{meas}(n) \right|^2} \tag{1.1}$$

Where N is the total number of samples of the input and output waveforms. Although NMSE is easy to calculate, it does not reflect accurately the model performance in the adjacent or out-of-band region of the spectrum.

1.5 Problem Statement and Objectives

Traditional methods for ETPA design do not take into account that the PA will be used in ET applications. In this thesis, a new method for ETPA design is proposed. The new

method develops a new criterion for the selection of the optimum load reflection coefficient and hence it takes into account the nature of the signal to be used and the shaping function to be applied in the envelope tracking system.

Unfortunately, ETPAs generate more nonlinearity because of their drain supply modulation making the conventional PA modeling techniques not suitable for them. In this thesis, a Volterra-series with compressed sampling based behavioral model is proposed for accurate modeling of ETPA nonlinearities. Moreover, for ETPA linearization, a two-box dual-input-single-output model has been proposed to mitigate the intensity of these nonlinearities.

The main objectives of this thesis are the following

- Coming up with a new approach for designing ETPA.
- System level simulation of the ETPA.
- Behavioral Modeling of the ETPA.
- Digital predistortion of the ETPA.

1.6 Thesis Organization

This thesis investigates the design, modeling, and linearization of envelope tracking power amplifiers. An introduction is provided in Chapter 1, along with a brief review about the constant bias PAs and the ETPAs and their operation principles. Also some light was shed on the basic principles of behavioral modeling, DPD, and the nonlinear distortions metrics. Then, the chapter ends by presenting the thesis objectives. Chapter 2

discusses different PA behavioral models and digital predistorters available in the literature. It summarizes all the studies that have been carried out in modeling and linearizing of ETPAs namely the main two models: single-input-single-output and dual-input-single-output models. Chapter 3 firstly discusses the problem of selection of the optimum load reflection coefficient that makes the PA operates at higher average efficiency when used in ET architecture. Then, it describes the details of designing envelope tracking path; and finally, it is concluded by performing a system level simulation for testing the ETPA characteristics. Chapter 4 starts with discussing the experimental setup used for performing the ETPA measurements, then it embarks in proposing new models for modeling and linearizing ETPA, and finally ends with comparing the proposed models with models in the literature. Finally, Chapter 5 contains the summary of the thesis, future work and potential extensions.

CHAPTER 2

LITERATURE REVIEW OF ETPA MODELING AND DIGITAL PREDISTORTION

Efficient and linear operation of RF power amplifiers is of prime importance as it is one of the most important components in wireless communication systems. Therefore, behavioral modeling, which attempts to predict the linearity performance of the power amplifier, has attracted the interest of many researchers over the past couple of decades. Because of the use of wide bandwidth signals, memory effects have become an essential part of power amplifier behavior along with the static nonlinearity and cannot be ignored. Numerous models have been described in the literature to depict the nonlinear behavior of power amplifiers driven by wide bandwidth signals. These structures include the memoryless look-up table model [14], Hammerstein and Wiener models [15]–[17], memory polynomial (MP) model and its modifications [12], [18]–[21] , twin-nonlinear two-box models [22], 3-box models such as PLUME model [23], generalized TNTB model [24], Volterra model and its variations [25]–[28].

A tremendous amount of research has been devoted to the problem of PA modeling, however, only few studies have actually shed some light on ETPA modeling problem

[34]-[46]. This could be referred to the fact that ETPA modeling problem is always accompanied by two common concerns. The first concern is that, the bandwidth of the envelope signal is 3-4 times larger than that of the RF modulated signal [29] which will make the process of designing envelope amplifier more difficult. The second one is the two input time alignment problem; where any time misalignment will degrade the efficiency and the linearity of the PA [30]. Furthermore, the dual-input nature of ETPA causes nonlinear distortions which need to be compensated for using special modeling techniques. Due to the importance of these problems and the crucial role that they play in determining the overall performance of the ETPA, several studies have been dedicated to them. In [31], a new method has been developed for generating suitable signals in terms of envelope speed for exciting the envelope amplifier, critically limited by its slew envelope. Furthermore, in [32], a method based on consecutive filtering processes is used to reduce the bandwidth of the modulated signal envelope and hence increases the efficiency of the envelope amplifier. However, the main limitation of this method is that the delay introduced by the filtering processes makes it unsuitable for real time applications. In [33], another method based on that introduced in [31] was developed, the new method can effectively reduce the envelope bandwidth but that comes at the cost of more complexity.

Dedicated modeling techniques for ET architecture have been proposed in [34]-[37]. Results have shown that the nonlinearity caused by modulating the drain voltage can be compensated for by using DPD techniques. A piecewise dynamic deviation reduction Volterra series-based modeling method [38] has been used for the ET architecture in [34]. However, details regarding the co-control of the input and envelope signals so that

maximum efficiency is achieved were not provided. On the other hand, linearization technique in [35] uses static characterization results as a basis for an efficiency-optimized co-control of the RF and envelope input signals. Then, a traditional DPD is used to compensate the nonlinear distortion and the residual memory effects. However, it is expected that the linearization performance of the transmitter will be limited due to the inaccuracies in the static model used in this method. Methods in [36] and [37] fully investigate the hybrid-envelope elimination and restoration (EER) transmitter (similar to the ET architecture). They have also developed a new linearization configuration as well as a co-control scheme for the modulated and envelope input signals. Improved efficiency and linearity figures have been achieved according to the experimental results.

Despite the importance of these efficiency enhancement PA architectures and the efforts that have been dedicated to linearize them, most of the works are in single-input-single-output basis. However, recently two research groups: Montoro *et al.* and Asbeck *et al.* have shed some light on new approaches that suit the dual-input-single-output nature of ET systems [40]-[46]. These methods are capable of providing superior performance compared with the single-input-single-output while considering the inevitable practical problems of envelope bandwidth and time misalignment sensitivity. However, this area is relatively new and a lot of contributions can be done here. The second sub-section explains the dual-input-single-output method and how it could be applied to the ET architecture, however, the first sub-section will be about the single-input-single-output models.

2.1 Single-Input-Single-Output PA Models

2.1.1 Memoryless/ Look-Up-Table Model

Figure 2.1 shows the memoryless look-up table (LUT) model. This LUT based behavioral model has been widely used in the past because it is easily implemented and is relatively simple [14]. This model does not include memory effects, and thus has a limited use now. In fact, currently, this model is used as a sub-model of more advanced structures that incorporate the memory effects of the power amplifier. In the LUT model, the gain of the device under test is saved in the look-up table. The LUT output is calculated as

$$x_{out}(n) = G\left(\left|x_{in}(n)\right|\right) \cdot x_{in}(n) \tag{2.1}$$

where $G\left(\left|x_{in}(n)\right|\right)$ represents the instantaneous gain of the DUT.

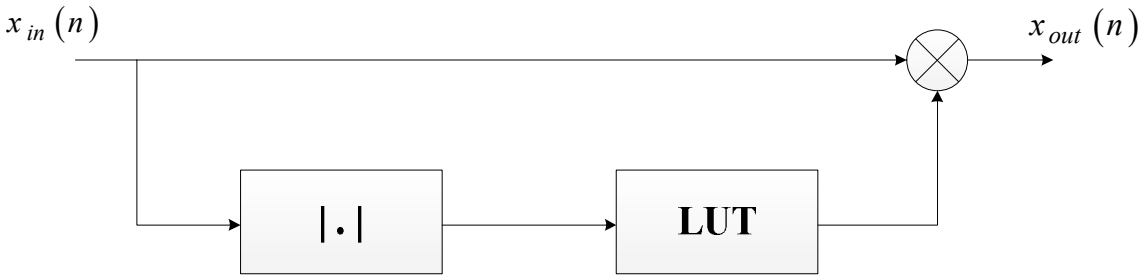

Figure 2.1: Block diagram of the look-up-table model [13]

2.1.2 Memory Polynomial Model (MP)

Memory polynomial (MP) model [12] consists of several delay taps and nonlinear static functions. Because of its simple structure and high accuracy, this model is extensively

used for behavioral modeling and digital predistortion applications of power amplifiers that exhibit memory effects. The memory polynomial model is given by:

$$y_{MPM}(n) = \sum_{j=1}^{M}\sum_{i=1}^{N} a_{ji}\, x_{in}(n+1-j)\cdot\left|x_{in}(n+1-j)\right|^{i-1} \tag{2.2}$$

where, $y_{MPM}(n)$ is the output of the memory polynomial model as shown in Figure 2.2, $x_{in}(n)$ is the complex input signal, N is the nonlinearity order and M represents the memory depth of the model. a_{ji} are the model coefficients which can be determined using least square approximation techniques.

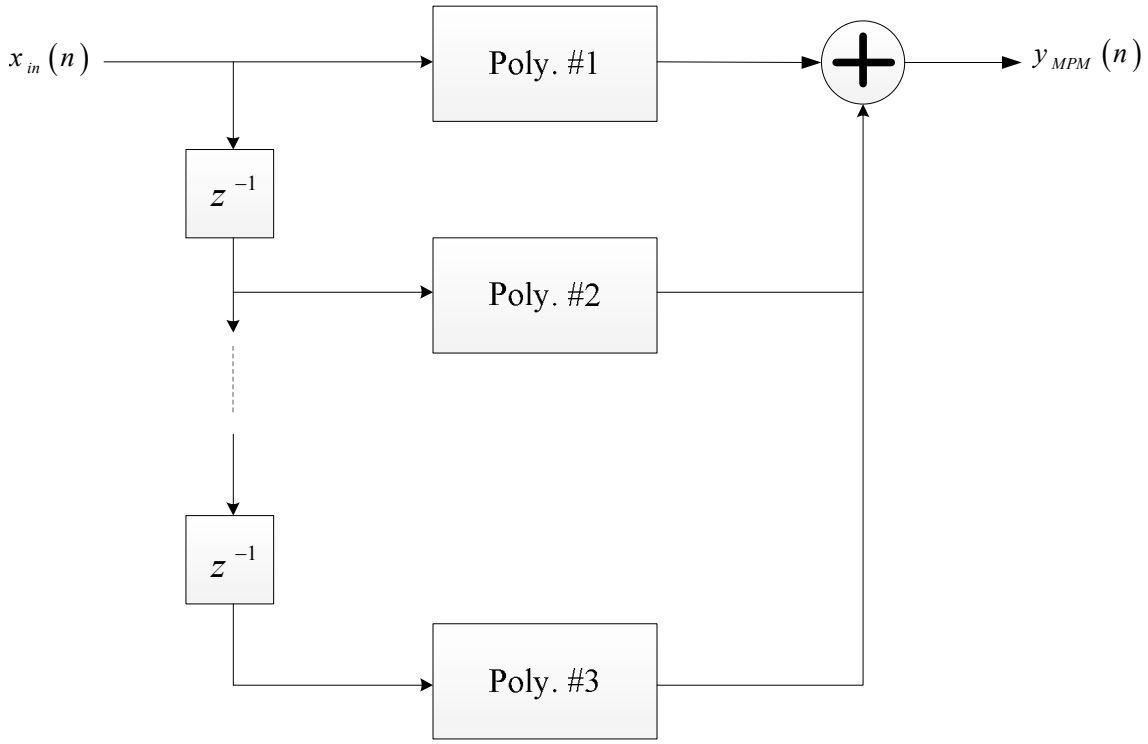

Figure 2.2: Block diagram of the memory polynomial model [13]

This model is a truncation of the Volterra model considering only the diagonal terms. The diagonal limitation significantly decreases the complexity, however it degrades model

fidelity as in particular cases the off-diagonal terms may influence the output in a significant manner [25]. Another disadvantage of the memory polynomial model is that same nonlinear order is used in all the branches leading to oversized which is undesirable [21].

2.1.3 Generalized Memory Polynomial Model (GMPM)

Combining the memory polynomial model in (2.2) with cross terms between the signal and its leading and lagging envelope terms results in the generalized memory polynomial model [20] described as

$$y_{GMP}(n) = \sum_{k=0}^{N_a-1}\sum_{m=0}^{M_a-1} a_{km}\, x(n-m)\left|x(n-m)\right|^k + \sum_{k=1}^{N_b}\sum_{m=0}^{M_b-1}\sum_{l=1}^{L_b} b_{kml}\, x(n-m)\left|x(n-m-l)\right|^k + \sum_{k=1}^{N_c}\sum_{m=0}^{M_c-1}\sum_{l=1}^{L_c} c_{kml}\, x(n-m)\left|x(n-m+l)\right|^k \tag{2.3}$$

Here, $x(n)$ and $y_{GMP}(n)$ are the input and output signals of the generalized memory polynomial model respectively. a_{km}, b_{kml}, c_{kml} represent the model coefficients of the MP branch, lagging effect branch and leading effect branch, respectively. M_a and N_a are the memory depth and the nonlinear order of the MP branch, respectively. M_b, M_c and N_b, N_c are memory depths and nonlinearity orders of the lagging and leading branches, respectively. L_b and L_c are the lagging and leading tap lengths, respectively. The generalized memory polynomial model does not separate the nonlinearity and memory effects, and hence all the memory branches use the same high nonlinearity order which results in undesirable high complexity. In order to model a highly nonlinear PA,

higher memory depth and nonlinearity order need to be used which increase the model complexity.

2.2 Envelope Tracking Power Amplifiers Models

ET systems possess an extra degree of freedom compared with the conventional fixed drain PAs [40]. This flexibility is utilized to improve the efficiency and linearity figures when input RF and envelope signals are designed properly. Figure 2.3 illustrates the general idea of dual-input representation of ET architecture.

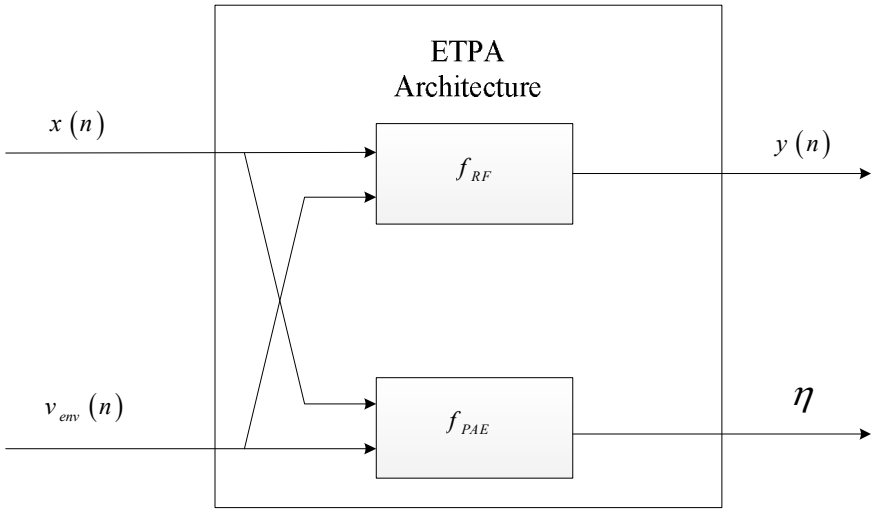

Figure 2.3: General concept of ET architecture [40].

Referring to the concept of operation of ETPA stated in section 1.2, the output RF signal, $y(n)$, and the PAE, η, are functions of the input RF signal $x(n)$ and envelope signal $v_{env}(n)$, respectively. Hence, the model is generated by

$$y(n) = f_{RF}\left(\mathrm{x}(n), \mathrm{v}_{env}(n)\right) \tag{2.4}$$

$$\eta = f_{PAE}\left(\left|\mathrm{x}(n)\right|, \mathrm{v}_{env}(n)\right) \tag{2.5}$$

As these two equations indicate, there can be many different combinations of $x(n)$ and $v_{env}(n)$ that can satisfy the first equation for a given $y(n)$. Thus, among all possible solutions, one has the flexibility to choose the combination of $x(n)$ and $v_{env}(n)$ that guarantees the highest PAE. This problem can be viewed as a constrained optimization problem to find the optimal input RF signal $x_{opt}(n)$ and the optimal envelope signal $v_{env-opt}(n)$, that can be best expressed as

$$\left(\mathrm{x}_{opt}(n), \mathrm{v}_{env-opt}(n)\right) = \underset{x, y_{env}}{\operatorname{argmax}} f_{PAE}\left(\left|\mathrm{x}(n)\right|, \mathrm{v}_{env}(n)\right) \tag{2.6}$$

$$\text{Subject to } f_{RF}\left(\mathrm{x}(n), \mathrm{v}_{env}(n)\right) = \mathrm{y}_{desired}(n) \tag{2.7}$$

where $y_{desired}(n)$ is the desired output signal of the power amplifier. On the interpretation of the equations (2.6) and (2.7), two approaches to linearize and/or model ETPAs have been developed; the static model and the dual input model.

2.2.1 Single-input-single-output ETPA Models

The basis of modern static model techniques is to jointly find the optimal input RF and envelope signals in order to achieve the maximum possible PAE and minimum distortion. All the dedicated linearization methods can be represented by Figure 2.4 and Figure 2.5, where f_1 is the static polynomial function of the RF input signal and f_2 is the static polynomial function of the envelope signal.

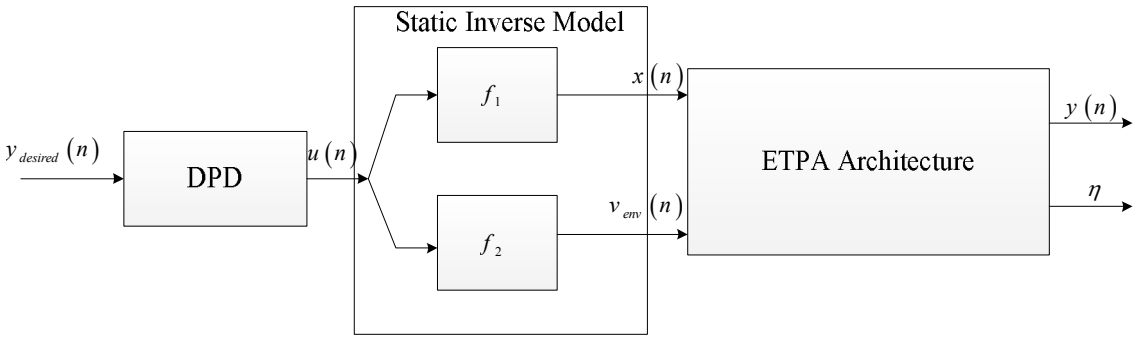

Figure 2.4: Linearization method in [35] and [39]

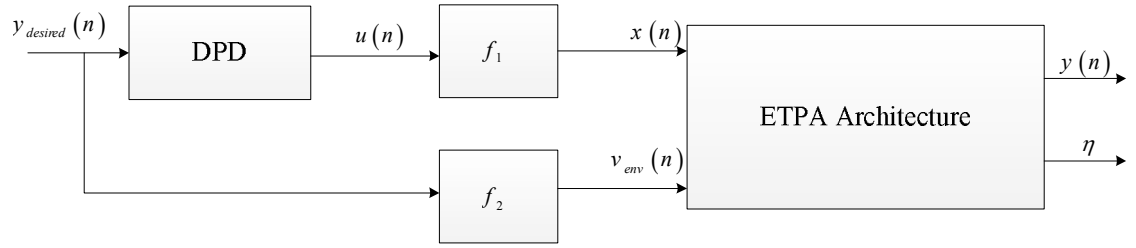

Figure 2.5: Modified linearization method in [35] and [39]

The following steps are used to derive the static model in [35] and [39]:

1- Perform a static power sweep measurements.

2- Use (2.7) to identify the efficiency optimized settings based on the measurements.

3- Construct the input RF and envelope signals with efficiency-optimized settings using the polynomial models.

One limitation of the static model is that it can only invert the nonlinearity of the ETPA to a limited extent and over fitting problems may occur if the polynomial order is increased. The DPD in Figure 2.4 cannot compensate for fitting errors that happen at both the baseband and RF branches. On the other hand, the DPD in Figure 2.5 can only

compensate for RF branch distortion since no knowledge is provided about the baseband branch errors. However, these errors will deteriorate the RF output signal linearity. Thus, the single-input (static) model illustrated by Figure 2.4 and Figure 2.5 cannot simultaneously optimize the efficiency and linearity of the ETPA.

2.2.2 Dual-input-single-output ETPA Models

In dual-input model the predistorted signal is constructed using the information from both the RF and the baseband branches. In [40], a two-step approach is followed instead of solving equations (2.6) and (2.7) jointly. The first step is to choose the envelope signal that maximizes the average PAE. The second step is to choose the RF input signal that can minimize the distortion between the desired RF $y_{desired}(n)$ and the RF $y(n)$ output signals. The fundamental point in this technique is that for any given $v_{env}(n)$ the PA can properly be predistorted as long as the DPD has knowledge of the chosen $v_{env}(n)$. Thus, for an appropriate given $v_{env}(n)$, the function in (2.4) can normally be inverted since it represents a one-to-one mapping between the RF input $x(n)$ and output $y(n)$. Then, the predistorted input signal can be written as

$$x(n) = f_{RF}^{-1}\left[\mathrm{y}(n), \mathrm{v}_{env}(n)\right] \tag{2.8}$$

where f_{RF}^{-1} represents the inverse function with respect only to $x(n)$ and $y(n)$ for a given $v_{env}(n)$. According to (2.8) the PA can be presistorted even if the $v_{env}(n)$ is non-optimally chosen, so, $v_{env}(n)$ can be constant or bandlimited. Furthermore, the condition

in (2.7) can be fulfilled by letting $y(n) = y_{desired}(n)$, and consequently the RF input signal will be

$$x_{opt}(n) = f_{RF}^{-1}\left[\mathrm{y}_{desired}(n), \mathrm{v}_{env}(n)\right] \tag{2.9}$$

Now, the RF input signal $x_{opt}(n)$ is only optimized for linearization operation and not efficiency optimized since $v_{env}(n)$ is non-optimally chosen. However, in order to maximize the efficiency, the variable $x(n)$ in (2.5) is replaced by $x_{opt}(n)$ in (2.9) and the efficiency-optimized envelope signal $v_{env-opt}(n)$ can be written as

$$\begin{aligned} v_{env-opt}(n) &= \arg\max_{v_{env}} f_{PAE}\left(\left|\mathrm{x}_{opt}(n)\right|, \mathrm{v}_{env}(n)\right) = \\ &\arg\max_{v_{env}} f_{PAE}\left(\left|\mathrm{f}_{RF}^{-1}\left(\mathrm{y}_{desired}(n), \mathrm{v}_{env}(n)\right)\right|, \mathrm{v}_{env}(n)\right) \end{aligned} \tag{2.10}$$

As (2.10) suggests, the optimal envelope signal $v_{env-opt}(n)$ which results in maximum efficiency of the ETPA is only a function of the desired output signal $y_{desired}(n)$ and it can be written as

$$v_{env-opt}(n) = g\left[\mathrm{y}_{desired}(n)\right] \tag{2.11}$$

Although the expression in (2.11) is simple, the identification of the function g can be quite difficult as it can be seen from (2.10). Having the optimum envelope signal $v_{env-opt}(n)$ in hand, the optimal predistorted input signal $x_{opt}(n)$ can directly be found from (2.9). A block diagram showing the dual-input model is shown in Figure 2.6.

The main disadvantage of this method is that, separate steps are needed to solve the efficiency optimization and distortion minimization problems.

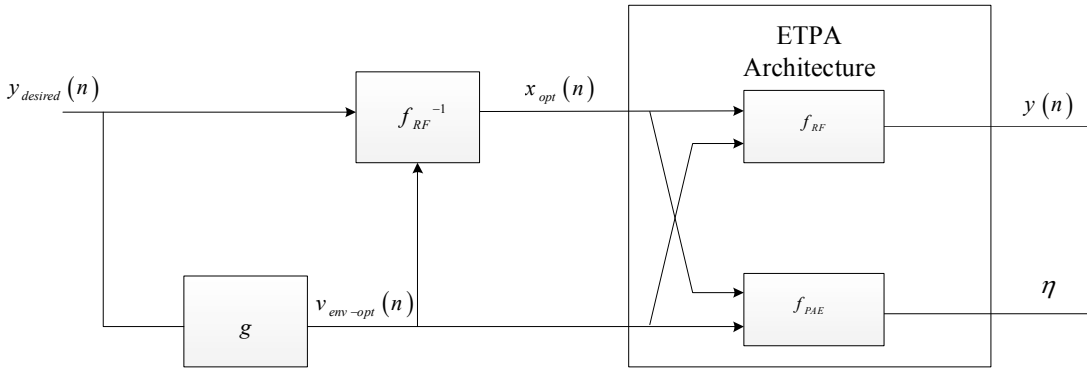

Figure 2.6: Dual input model for ETPA [40].

The efficiency-optimized function g shown in (2.11) is modeled as a polynomial function and it is formulated as

$$v_{env}(n) = g\left[\mathrm{y}(n)\right] = \sum_{k=0}^{K} a_k \left|y(n)\right|^k \tag{2.12}$$

where $\mathrm{y}(n)$ is the RF output signal, K is the nonlinearity order, and a_k are the model coefficients.

However, the dual input function f_{RF}^{-1} can be modeled by the same single-input-single-output behavioral model with one more real-valued dimension corresponding to the envelope signal $v_{env}(n)$. In [40], a modified 2-D GMP has been developed based on the GMP model [20] and used for dual-input-single-output behavioral model. The DPD function f_{RF}^{-1} is written as

$$x(n) = f_{RF}^{-1}\left(\mathrm{y}(n), \mathrm{v}_{env}(n)\right) = \sum_{n_1=1}^{N_1}\sum_{m_1=0}^{M_1}\sum_{m_v=0}^{M_v}\sum_{p=0}^{P} h_{n_1 m_1 m_v, p}\, y_{m_1}(n)\left|y_{m_1}(n)\right|^{n_1} v_{env,m_v}^{p}(n)$$
$$+\sum_{n_2=1}^{N_2}\sum_{m_2=0}^{M_2}\sum_{l_1=0}^{L_1}\sum_{m_v=0}^{M_v}\sum_{p=0}^{P} h_{n_2 m_2 l_1 m_v, p}\, y_{m_2}(n)\left|y_{m_2+l_1}(n)\right|^{n_2} v_{env,m_v}^{p}(n)$$
$$+\sum_{n_3=1}^{N_3}\sum_{m_3=0}^{M_3}\sum_{l_2=0}^{L_2}\sum_{m_v=0}^{M_v}\sum_{p=0}^{P} h_{n_3 m_3 l_2 m_v, p}\, y_{m_3}(n)\left|y_{m_3-l_2}(n)\right|^{n_3} v_{env,m_v}^{p}(n)$$

(2.13)

Where N is the nonlinearity order, M is the RF input signal memory depth, L is the leading/lagging memory depth, M_v is the envelope signal memory depth, P is the envelope signal nonlinearity order, h are the model coefficients for the 2-D GMP model, $y_m(n)$ represents output RF signal with delay m, $y(n-m)$, and $v_{env,m_v}(n)$ is the envelope signal with delay m_v, $v_{env}(\mathrm{n}-\mathrm{m}_v)$. One can notice that, the new behavioral model has one more input than the normal single-input PA behavioral models. Consequently, the dual-input model can utilize this new input in constructing the predistorted RF input signal. Unlike static models, this model can compensate for fitting errors caused when deriving the optimal envelope signal -if any- through the predistorted RF signal.

In [40], the bandwidth reduction technique developed in [29] was used to generate 5.6 MHz reduced-bandwidth envelope signal. As it is well established, additional memory effects might be introduced because of the use of the reduced-bandwidth envelope signal [41]. However, the dual-input DPD should be able to mitigate these memory effects since the RF predistorted signal is now constructed using the reduced-bandwidth envelope signal. In other words, the constructed predistorted RF signal is still linearity-optimized,

however, the average PAE will be degraded since the reduced-bandwidth envelope signal is not the efficiency-optimized signal anymore. The DUT in [40] is a varactor-based dynamic load modulation (DLM) PA (similar to ETPA) operating at 2.65 GHz [42][43] with a peak output power of 38 dBm. A single carrier WCDMA signal with 7 dB PAPR is used as an input signal to the PA. The dual-input technique in [40] is compared with the static models in [42] and [43] as shown in Table 2.1.

Table 2.1: Comparison of Different Linearization Methods[40]

Methods	PAE [%]	Power [W]	NMSE	ACLR1[dB]	# of Coeff.
Method in [42]	48	1.2	-32	-41	100
Method in [43]	49	1.2	-34	-44	100
Method in [40]	49	1.2	-39	-50	200

As it can be seen, the proposed linearization technique simply outperforms the static linearization techniques and can effectively be used to minimize the amount of distortion and maximize the PAE, however, the main limitation of this method is the huge number of coefficients (twice) needed compared with the static methods.

In [43], a behavioral model for ETPA has been developed where the envelope signal is slew-rate limited as suggested by the study in [31] so that the slew-rate requirements of the envelope amplifier are relaxed. In fact, when using slower envelope signal, nonlinearities will be introduced in the resulting amplified signal due to the time-variant gain effects. The authors in [44] have developed an envelope-dependent (ED) behavioral

model and its performance has been compared with that of the static model. The output complex baseband signal, $y_A(n)$, of a constant drain PA can be expressed as a function of the input complex baseband signal, $\mathrm{x}_A(n)$, and the relationship could be formulated as

$$y_A(n) = g_A\left(\left|\mathrm{x}_A(n)\right|\right)\cdot \mathrm{x}_A(n) \tag{2.14}$$

where $g_A(\cdot)$ is a function of the input signal envelope, $\left|\mathrm{x}_A(n)\right|$, only and constitutes the AM/AM and AM/PM characteristics

$$g_A\left(\left|\mathrm{x}_A(n)\right|\right) = g_A^{AM}\left(\left|\mathrm{x}_A(n)\right|\right)\cdot \mathrm{e}^{jg_A^{PM}\left(\left|\mathrm{x}_A(n)\right|\right)} \tag{2.15}$$

The static nonlinear modulus $g_A^{AM}(\cdot)$ and the phase of the gain $g_A^{PM}(\cdot)$ can be modeled as polynomials according to

$$g_A^{P}\left(\left|\mathrm{x}_A(n)\right|\right) = \sum_{i=0}^{N_1} c_i^{P}\cdot\left|\mathrm{x}_A(n)\right|^i \tag{2.16}$$

where $g_A^{P}(\cdot)$ can be either $g_A^{AM}(\cdot)$ or $g_A^{PM}(\cdot)$ and the model coefficients c_i^{P} can also be either c_i^{AM} or c_i^{PM}. However, when considering slower envelopes, these coefficients c_i^{P} are not constant and they depend on the slower envelope, $E_s(n)$, and thus these coefficients are replaced by a function $f_i^{P}\left(\mathrm{E}_s(n)\right)$ that depends on $E_s(n)$ as follows

$$g_A^{P}\left(\left|\mathrm{x}_A(n)\right|\right) = \sum_{i=0}^{N_1} f_i^{P}\left(\mathrm{E}_s(n)\right)\cdot\left|\mathrm{x}_A(n)\right|^i \tag{2.17}$$

where $f_i^P\left(\mathrm{E}_s\left(n\right)\right)$ is modeled as a polynomial function using

$$f_i^P\left(\mathrm{E}_s\left(n\right)\right)=\sum_{j=0}^{N_2}\gamma_{ij}^P\cdot\left(\mathrm{E}_s\left(n\right)\right)^j \tag{2.18}$$

The ED model coefficients are defined around the most probable $E_s\left(n\right)$ value (this can be obtained by calculating the statistical mode of histogram of the $E_s\left(n\right)$ values resulting in signal envelope nominal value E_s^{Nom}) in order to reduce the error due to the finite terms of the polynomial expansion (of orders N_1 and N_2). Therefore, the ETPA gain is formulated as incremental around the nominal gain function as

$$g_A^P\left(\left|\mathrm{x}_A\left(n\right)\right|,\mathrm{E}_s\left(n\right)-\mathrm{E}_s^{Nom}\right)=\sum_{i=0}^{N_3}\gamma_{i0}^P\cdot\left|\mathrm{x}_A\left(n\right)\right|^i+\sum_{j=1}^{N_2}\sum_{i=0}^{N_1}\gamma_{ij}^P\cdot\left|\mathrm{x}_A\left(n\right)\right|^i\cdot\left(\mathrm{E}_s\left(n\right)-\mathrm{E}_s^{Nom}\right)^j \tag{2.19}$$

Two parts can be differentiated from the above equation: a static nonlinear gain part (coefficients γ_{i0}^P) that depends on the input signal only, and a nonlinear time-variant gain part (coefficients $\gamma_{ij}^P, j\neq 0$) that depends on the input signal and the slow envelope signal.

In [45], the authors developed the DPD function corresponding to the aforementioned behavioral model. The DPD block diagram is shown in Figure 2.7.

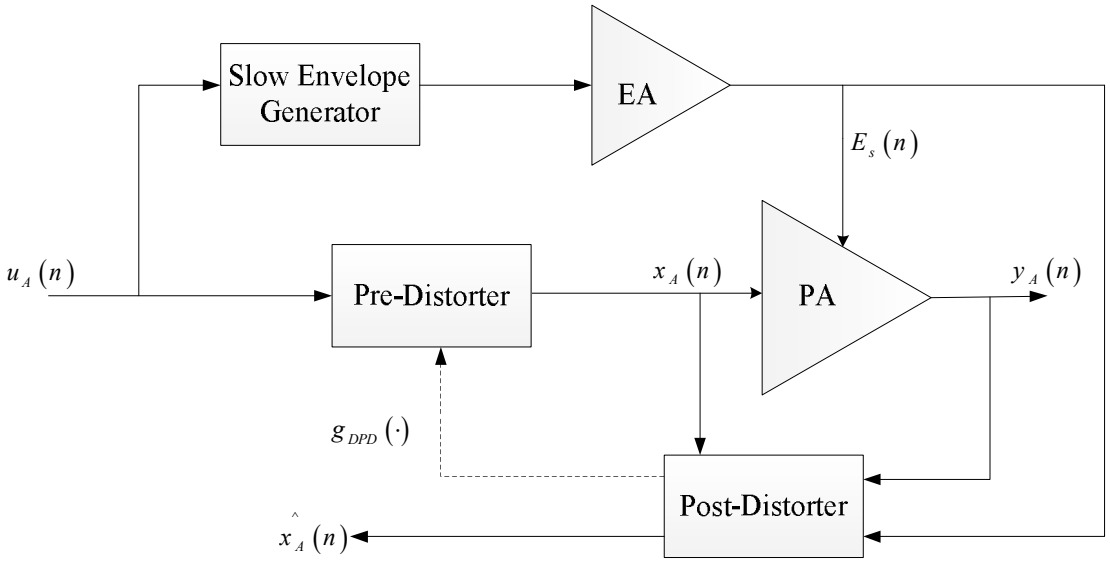

Figure 2.7: Block diagram of the DPD indirect learning approach [45]

where the post-distortion function is copied into the predistorter. The input and output relationship in the DPD could be written as

$$x_A(n) = g_{DPD}\left(\left|u_A(n)\right|, \mathrm{E}_s(n)\right) \cdot u_A(n) \tag{2.20}$$

Where

$$g_{DPD\_P}\left(\left|u_A(n)\right|, \mathrm{E}_s(n) - \mathrm{E}_{s\_Nom}\right) = \sum_{i=0}^{N_3} \gamma_{i0}^{DPD\_P} \cdot \left|u_A(n)\right|^i + \sum_{j=1}^{N_2} \sum_{i=0}^{N_1} \gamma_{ij}^{DPD\_P} \cdot \left|u_A(n)\right|^i \cdot \left(\mathrm{E}_s(n) - \mathrm{E}_{s\_Nom}\right)^j \tag{2.21}$$

The DUT in [44] and [45] was a PA designed using the CGH40006P_TB GaN transistor and operating at 2 GHz. 16-QAM OFDM based signals were used as test signals with a maximum envelope voltage of 28V. Table 2.2 and Table 2.3 present a comparison between static and the ED model and DPD, respectively.

Table 2.2: Static and ED Model for Different Sets of Coefficients[44]

Model	γ_{i0}	$\gamma_{ij}, j \neq 0$	NMSE [dB]	ACEPR [dB]
Static model	12		-26.1	-33.5
ED model #1	6	6	-35.4	-42.3
ED model # 2	6	12	-36.5	-43.5

Table 2.3: Static and ED DPD for Different Sets of Coefficients[45]

Model	# of coeff.	NMSE [dB]	ACEPR [dB]
Static DPD	9	-28	-29
ED DPD #1	9	-34	-37
ED DPD #2	16	-35	-38

As it can been seen, the developed model and DPD shows better linearization results compared with static model and DPD. The NMSE and ACEPR have proved the accuracy of the ED model and the ED-DPD in reproducing the unwanted time-variant nonlinear behavior and linearizing the slew-rate limited ETPA. However, these two studies address the problem of modeling and linearizing ETPA from only linearity perspective and it does not pay attention to the efficiency degradation caused by the slew-rate limited envelope signal. To be more specific, authors in [45] have not provided any information about how to co-control the envelope and the RF input signals so that maximum efficiency and best linearity could be reached at the same time. One more disadvantage,

[44] and [45] use memoryless polynomial model which is very simple. However, it is well-known in the literature that memory polynomial models performance is better than that of the memoryless polynomial models because of the former ability to accurately model and linearize the memory effects introduced by the PA when excited by wide bandwidth signals.

The model in [45] has been modified in [46] to compensate for memory effects by using a memory polynomial model. The block diagram used this time is similar to the one in [45] and it is shown in Figure 2.8. In fact, the only difference between the two methods is that, in [46], the generation of the slow envelope signal, E_s, is taking place before the predistortion block to avoid dealing with bandwidth expansion that will occur on the baseband complex signal after predistortion.

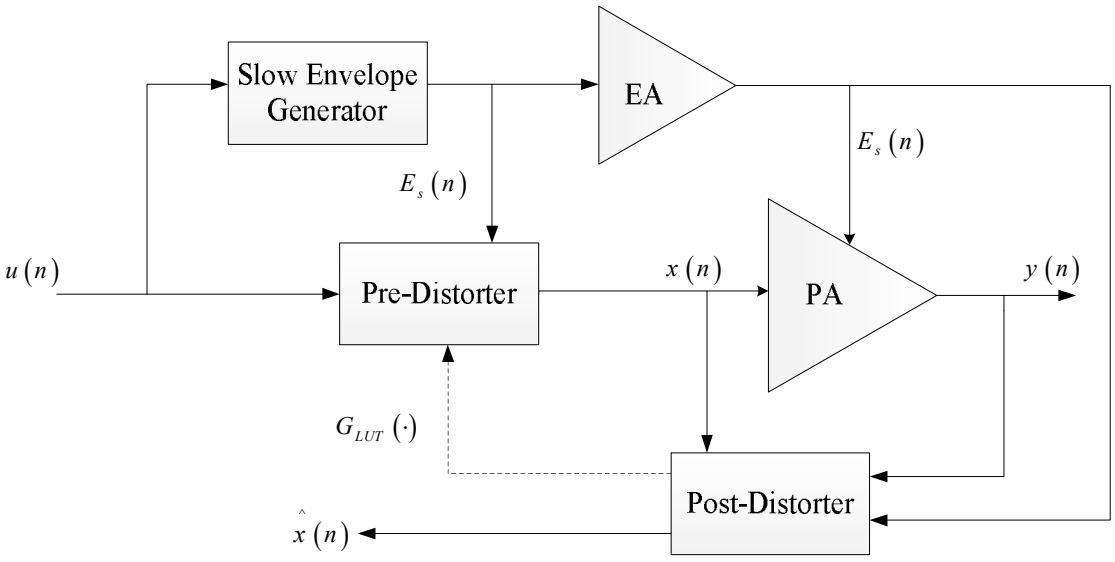

Figure 2.8: Block diagram of the DPD indirect learning approach [46]

Again the slew-rate limited envelope signal in [31] is used to relax the envelope requirements of the signals, and consequently the input and output relationship of the slow envelope dependent digital predistorter (SED-DPD) is defined as

$$x(n)=\sum_{j=0}^{M}\sum_{q=0}^{Q}\sum_{i=0}^{N}\sum_{p=0}^{P}\gamma_{piqj}\cdot\left[\mathrm{E}_s\left(\mathrm{n}-\tau_j\right)-\mathrm{E}_s^{Nom}\right]^q\cdot u\left(\mathrm{n}-\tau_j\right)\cdot u\left(\mathrm{n}-\tau_j\right)^p \tag{2.22}$$

where τ_i and τ_j (with $\tau_0=0$) are the most significant tap delays for the input signal and envelope signal, respectively. The SED-DPD is used to linearize ETPA (the same one in [44] and [45]) that is excited by three different signals with different bandwidths as seen in Table 2.4.

This table compares four types of linearization methods; the dynamic DPD (DPD with no knowledge about the slow envelope signal) has very poor performance whereas the memoryless SED-DPD proposed in [45] has better performance in terms of linearity. However, the dynamic SED-DPD shows better in-band distortion compensation compared with the memoryless SED-DPD and it maintains this advantage when wideband signals are used. Again, the main limitation of method in [46] is that it neglects the PAE degradation problem caused by using slow envelope signal and discusses the ETPA problem from only linearity point of view.

Table 2.4: Comparison of Different DPD Strategies [46]

Model	**WCDMA** $BW = 3.84MHz, SR_{red} = 88\%$		**One Carrier 64-QAM** $BW = 6.4MHz, SR_{red} = 96\%$		**OFDM 16-QAM** $BW = 10MHz, SR_{red} = 96\%$	
	NMSE (dB)	ACPR (dB)	NMSE (dB)	ACPR (dB)	NMSE (dB)	ACPR (dB)
No DPD	-10.4	-25.6/-25.6	-16.3	-35.8/-36.2	-14.1	-32.3/-33.0
Dynamic DPD	-17.7	-27.9/-28.8	-20.0	-35.1/-35.0	-17.4	-30.1/-29.5
Memoryless SED-DPD	-29.0	-30.5/-31.1	-29.9	-50.6/-50.6	-24.3	-38.2/-38.6
Dynamic SED-DPD	-30.7	-30.5/-31.5	-39.1	-51.0/-52.4	-35.5	-38.4/-39.7

2.3 Summary and Discussion

In this chapter, different models and DPD methods used for modeling and linearizing conventional and ET power amplifiers have been discussed. In fact, the chapter started by exploring various models used for modeling conventional constant drain supply power amplifiers. Then, a literature review of different models used for modeling and linearizing envelope tracking power amplifiers was demonstrated. Unlike conventional PAs, the drain supply represents an extra degree of freedom in ETPAs which might lead to an improved linearity for ETPA if it is incorporated wisely in the ETPA model.

CHAPTER 3

DESIGN METHODOLOGY AND SYSTEM LEVEL SIMULATION OF ENVELOPE TRACKING POWER AMPLIFIERS

In order to successfully design power amplifiers, specific design steps should be followed. However, one of the most important steps is to design output matching network; that totally depends on the accurate selection of the load reflection coefficient. Traditionally, there is no difference between the selection algorithms followed for either constant or variable supply (ET) PAs.

In this Chapter, the conventional method for selecting load reflection coefficient is described. Then, a new methodology for selecting optimum load reflection coefficient for ETPAs is presented in the second section of this chapter. Finally, a system level simulation for ETPA is described in the third section of this chapter.

3.1 Conventional Power Amplifiers Design Approach

Usually a list of the transistor's optimum source and load impedances are specified in the data sheet of the transistor by the transistor manufacturer. This list is usually specified experimentally at different frequencies and under specific operating points. Thus, if it is intended to design the PA under one of these same manufacturer conditions the problem is reduced into converting the load and source impedances to the ones provided by the manufacturer. However, in this thesis, these load impedance values cannot be directly

used because the biasing points and the frequency for which the PA is designed are different from those specified by the manufacturer. Consequently, using the transistor model (Cree CGH40010F) given by the manufacturer, the load pull method was used to design the class AB power amplifier.

Traditionally, the selection of the optimum load impedance is carried out using the load-pull procedure developed by Cripps back in 1983 [2][47]. The idea is to simply sweep the load impedances Z_L and continuously measure the output power and the PAE until the optimum value of Z_L that gives best values of output power and PAE is reached.

Figure 3.1 shows a practical method to simulate the optimum load impedance at a frequency of 2.14 GHz and available input power $P_{avs} = 27$ dBm which represents the maximum input power beyond which the transistor will saturate under the biasing conditions.

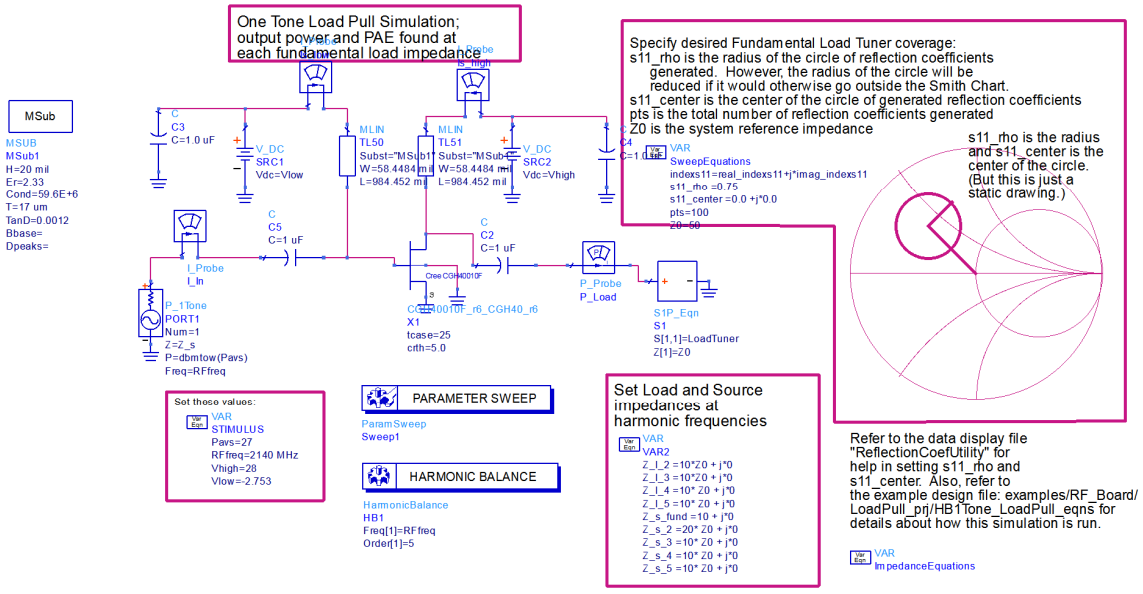

Figure 3.1: Conventional load pull setup.

The circular region of the smith chart specified by the radius and the center point is sampled in a certain way so that different load reflection coefficients located with this delimited area (and consequently impedances) are presented at the output of the transistor. For each reflection coefficient, the PAE and the power delivered (P_{del}) to the load are calculated and then the resultant PAE and P_{del} contours are plotted as shown in Figure 3.2. The PAE and P_{del} contours show the load impedances over which constant PAE and P_{del} are achieved, respectively.

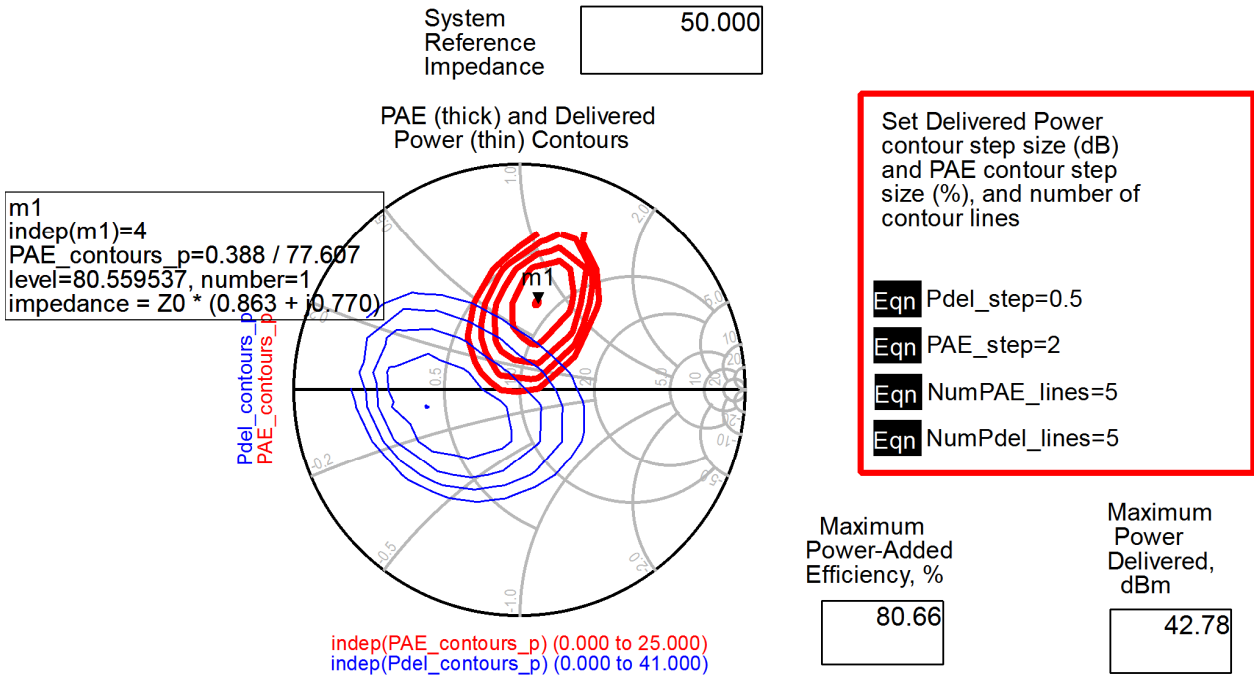

Figure 3.2: PAE and Pdel contoursPAE and Pdel contours.

In general, all the PAE and P_{del} contour intersection points are possible load impedance choices but usually in designing power amplifier, either maximum PAE or maximum P_{del} are targeted. In this thesis, maximum PAE is targeted, hence, the optimum load reflection coefficient value that lies in the intersection of the PAE and P_{del} contours and

results in maximum PAE and a reasonable P_{del} has been chosen. This approach shows how conventionally load impedance is chosen in order to design a PA. Instead of using this method, a novel method is introduced which takes into consideration that the PA will be used in an ET system.

3.2 Proposed Approach

This method was made based on the use of the power amplifier in an envelope tracking system and thus takes into account the nature of the signal to be used and the shaping function to be applied in the envelope tracking system. Thus a modified load-pull technique was utilized in which three sweeps have been carried out. Firstly, the load reflection coefficient was swept and a total of 100 reflection coefficients had been presented at the output of the CGH40010 transistor by the load tuner. Then, the driving input signal power (P_{avs}) was swept between (-10 and 27 dBm). Finally, the outer sweep utilized the drain voltage (V_{ds}) in order to simulate the envelope tracking mechanism since in ET the drain supply voltage is varying according to the input signal. The drain voltage swing range was set to (10 – 30V) to mimic the output of Nujira envelope modulator. Then, PA characteristics such as output power, PAE, and gain were captured for further processing. Figure 3.3 shows a block diagram of the proposed method algorithm where the shaping function was used to map the envelope of a modulated signal to the corresponding drain voltage.

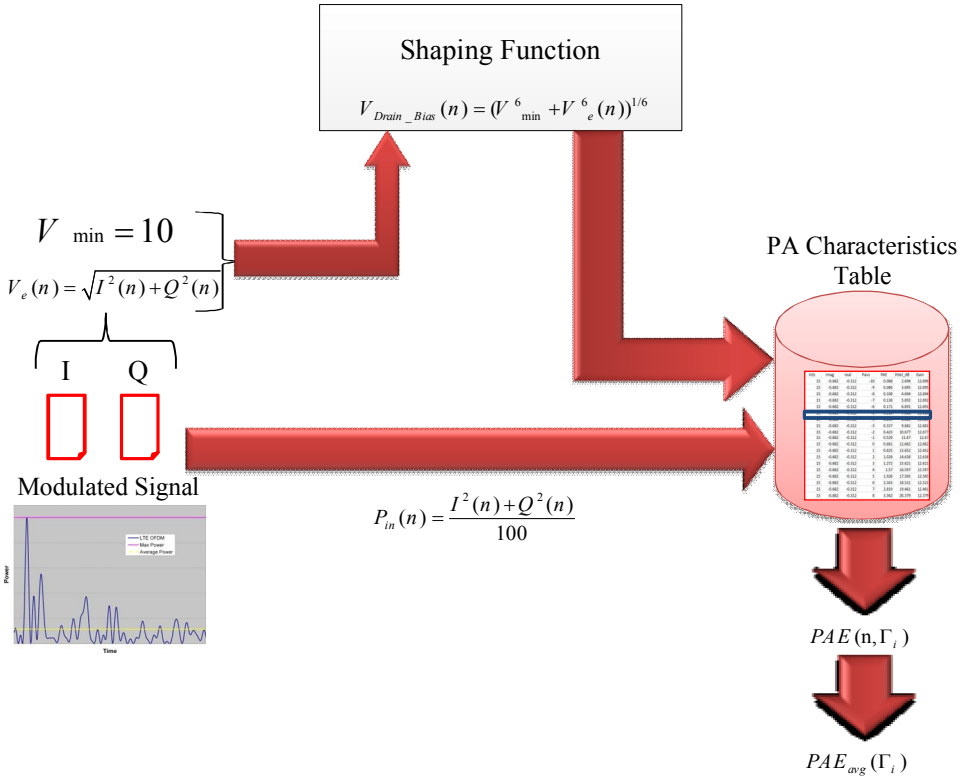

Figure 3.3: Block diagram of the proposed method for one Gamma.

With the PA characteristics table in hand, the working principle of the diagram shown in Figure 3.3 is better explained by the flowchart depicted in Figure 3.4. This flowchart shows the proposed process for only one Gamma. The process is repeated for the rest of the Gammas and the one Gamma that results in the maximum average PAE is selected to be the optimum value of the reflection coefficient. The proposed method described above was used to find the optimum load reflection coefficients when two different shaping functions are used in the envelope tracking path namely; Nujira N6 and Nujira-Wilson shaping functions [48] which are given by:

$$V_{Drain\_Bias}(n) = \left[V^{6}_{\min} + V^{6}_{e}(n)\right]^{1/6} \tag{3.1}$$

$$V_W(n) = \mathrm{V}_{\min}\left(\frac{\pi}{\pi-2}\right)\left[1-\left(\frac{2}{\pi}\right)\cos\left[V_e(n)\frac{(\pi-2)}{2V_{\min}}\right]\right] \tag{3.2}$$

Conventionally, load-pull setup is done without sweeping the drain voltage then the load reflection coefficient which results in maximum PAE is selected to be the optimum one. However, in order to carry out a fair comparison with the proposed method an averaged version of the conventional method was used to obtain the optimum reflection coefficient as in Figure 3.5.

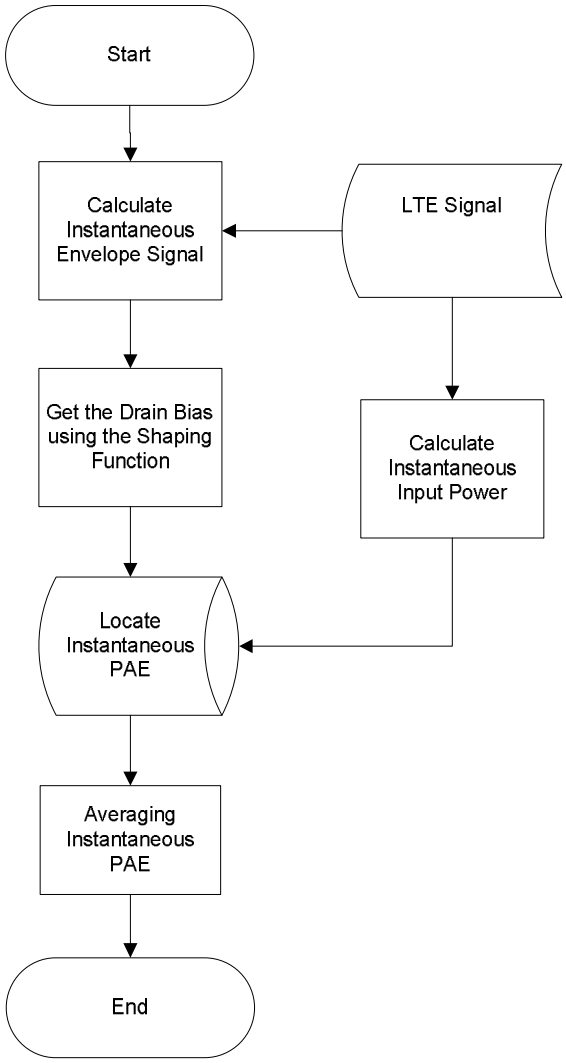

Figure 3.4: Proposed method flowchart for a single Gamma.

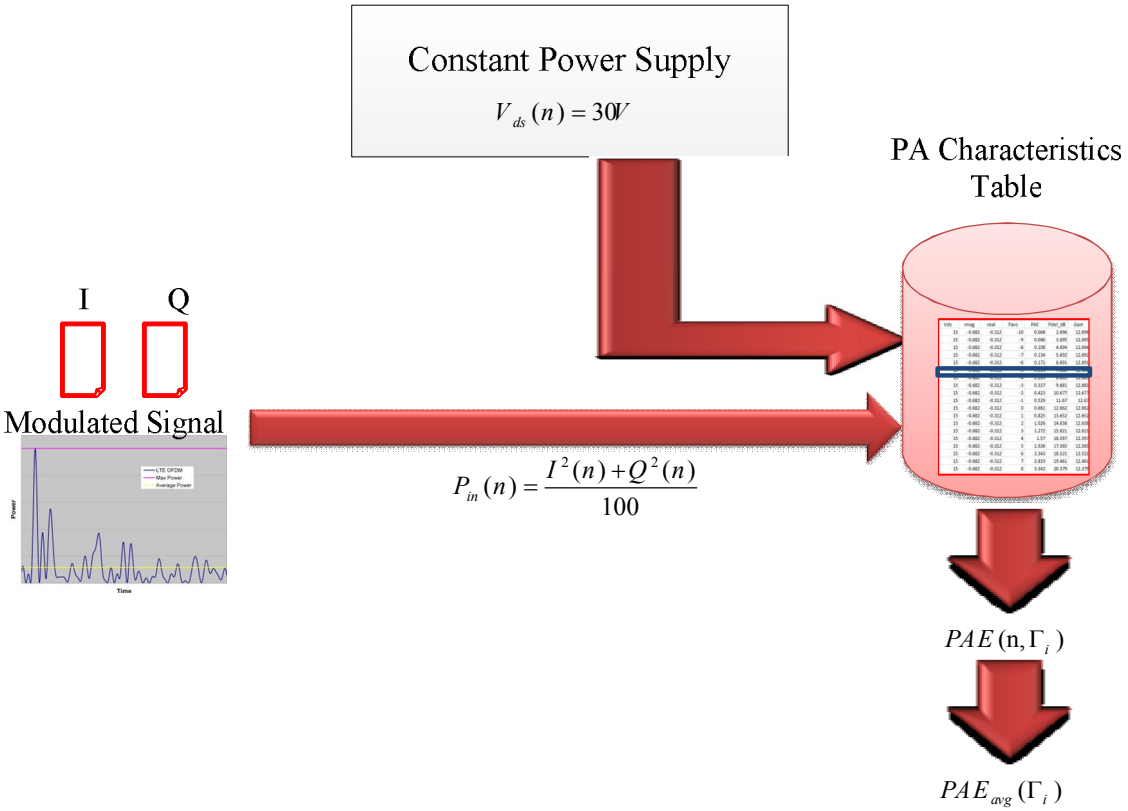

Figure 3.5: Conventional constant supply averaged approach.

A Cree CGH40010 10-Watt transistor was used for the PA design around 2.14 GHz. An LTE signal centered at 2.14 GHz with a PAPR of 10.04 dB and 20 MHz bandwidth was used as an input signal to the system.

The PAE contours for fixed and variable drain bias are shown in Figure 3.6 and Figure 3.7 for Nujira N6 and NujiraWilson shaping functions, respectively. As it can be noticed in both figures the PAE levels achieved using variable drain bias are higher than those of constant V_{ds} as expected.

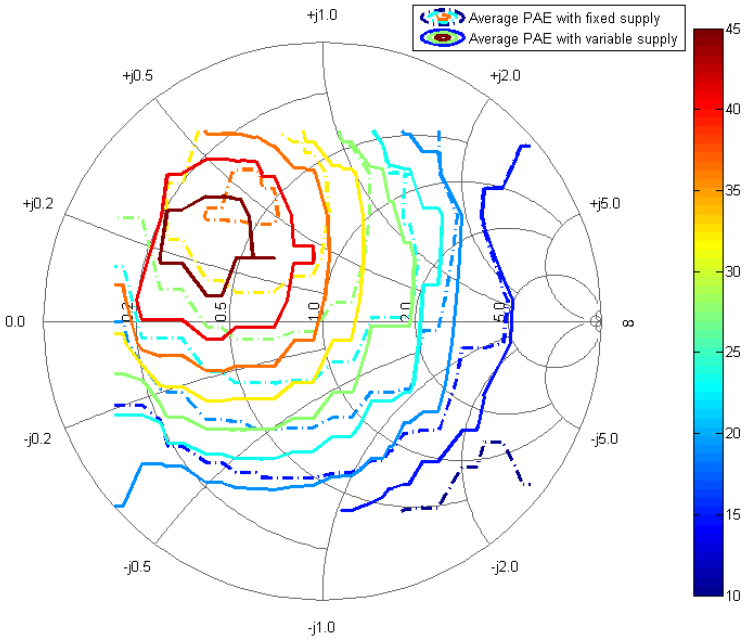

Figure 3.6: PAE contours for fixed and variable Nujira N6 drain bias.

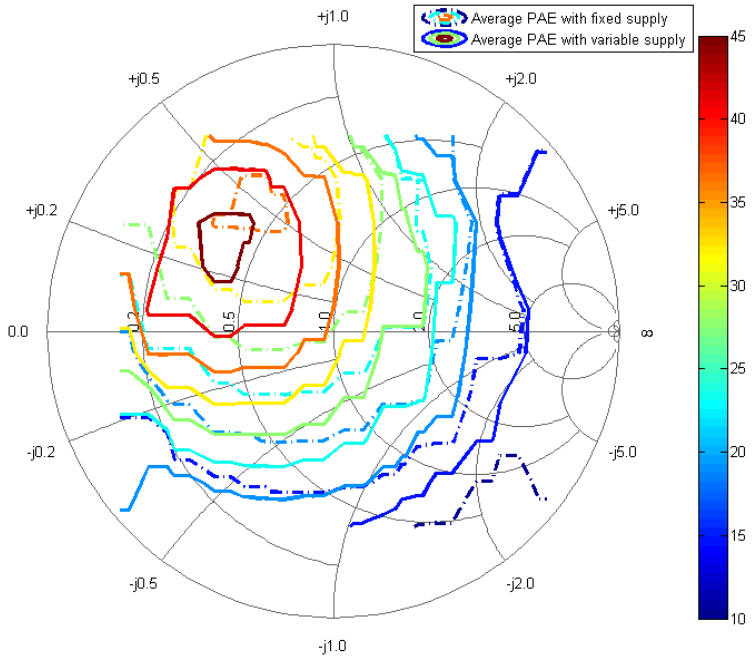

Figure 3.7: PAE contours for fixed and variable Nujira-Wilson drain bias.

Furthermore, in both figures, there is a shift between centers of the variable and constant V_{ds} contours indicating that their maximum PAEs occur for different reflection coefficient values. The optimum load reflection coefficient value for fixed supply PA was found to be -0.216 + 0.379j and it led to 35.45% maximum average PAE. However, for variable supply PA the optimum load reflection coefficient was found to be -0.397 + 0.227j resulting in 47.27% maximum average PAE when Nujira N6 was used for modulating drain bias. For Nujir-Wilson modulated drain bias, the optimum load reflection coefficient value was -0.397 + 0.227j which resulted in 46.02% maximum average PAE. The above mentioned results are summarized in Table 3.1 for comparison purposes.

Table 3.1: Optimum Reflection Coefficients Results

Shaping Function	**Optimum Reflection Coefficient**		**Average PAE**	
	Conventional	Proposed	Conventional	Proposed
Nujira N6	-0.216 + 0.379j	-0.397 + 0.227j	44.18%	47.27%
NujiraWilson	-0.216 + 0.379j	-0.397 + 0.227j	43.46%	46.02%

Table 3.1 also shows that, if the optimum Gamma is selected using the traditional method (i.e. the fixed drain optimum Gamma is selected which is (-0.216 + 0.379j)), 44.18% and 43.46% maximum average PAEs will be achieved using Nujira N6 and NujiraWilson shaping functions, respectively. On the other hand, if the new approach is followed, 47.27% and 46.02% maximum average PAEs could be achieved using Nujira N6 and NujiraWilson shaping functions, respectively. Thus, around 3% increase in the average

PAE was obtained for both shaping functions by only following the proposed approach. This improvement in PAE is costless since it is only concerned by optimally choosing the load reflection coefficient and hence there is no additional hardware complexity. The simulation results reveal that, NujiraWilson tends to have lower efficiency figures when compared with Nujira N6, as supported in [48]. With the optimum load reflection coefficient in hand, the output matching network has been designed and the overall PA has been implemented.

Figure 3.8 shows the drain efficiencies of both the fixed supply PA and the ETPA together with input and output signals probability density functions (PDF). Both the ETPA and the fixed supply PA were implemented using the proposed method optimum reflection coefficients and all the PAE figures have been confirmed.

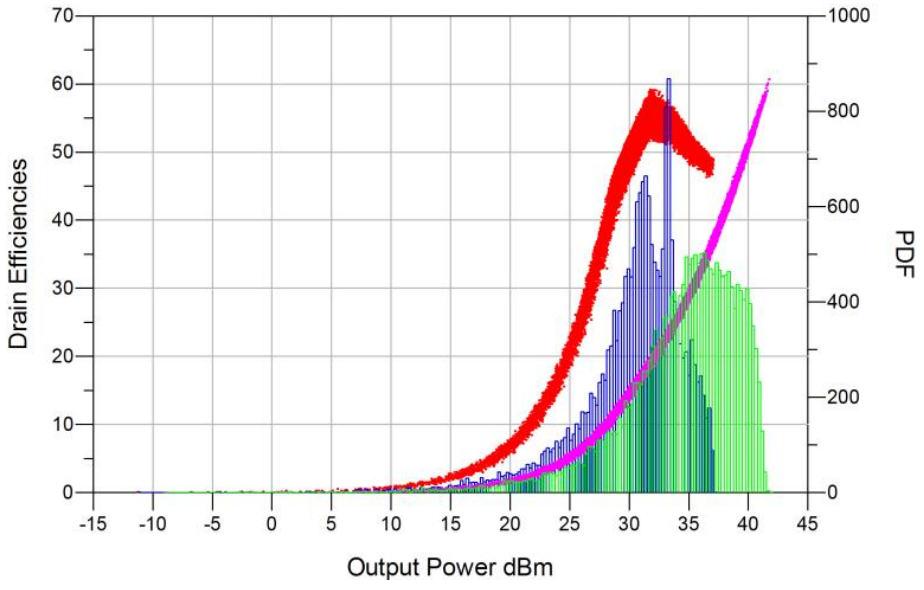

Figure 3.8: Fixed supply PA and ETPA PAEs with the signals PDFs.

3.3 System Level Simulation of Envelope Tracking Power Amplifiers

In order to accurately model and consequently predistort envelope tracking power amplifiers, it is very important to have an idea about the nonlinearities than can be caused in such types of power amplifiers. System level simulation of ETPAs will act as the perfect environment to identify such nonlinearities and it will give us the perfect opportunity to mitigate them through digital predistorters.

This section is about implementing a system level simulation of ETPA. It starts with designing the envelope path of the ETPA. Then, based on the optimum load provided in the previous section, a PA is implemented and the designed ETPA path will be attached to it. The ETPA overall performance in terms of average PAE, AM/AM, and AM/PM will be demonstrated.

3.3.1 Envelope Tracking Path Design

Figure 3.9 shows a block diagram for an ETPA. In this design, the input signal power sampling and drain voltage shaping and modulation operations are performed using ideal behavioral components, however non-idealities could be introduced.

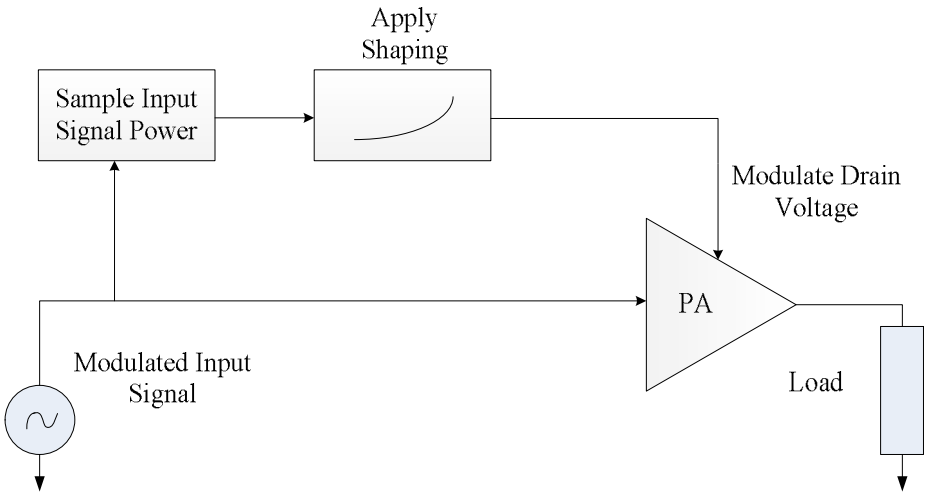

Figure 3.9: ETPA block diagram.

As Figure 3.9 suggests, several steps are needed to design ETPA. These steps could be summarized as:

1- Generate a modulated signal.

2- Implement a method for sampling the input signal power.

3- Determine the shaping function to be used.

4- Implement a method for modulating the drain bias voltage.

In this thesis, a baseband LTE signal represented by I and Q text files was considered. ADS was used to generate an LTE signal waveform with 20 MHz bandwidth centered around 2.14 GHz.

The signal spectrum and complementary cumulative distribution function (CCDF) are shown in Figure 3.10. Having the modulated signal ready, one should find a way to reuse this signal in the simulation and then detect its power.

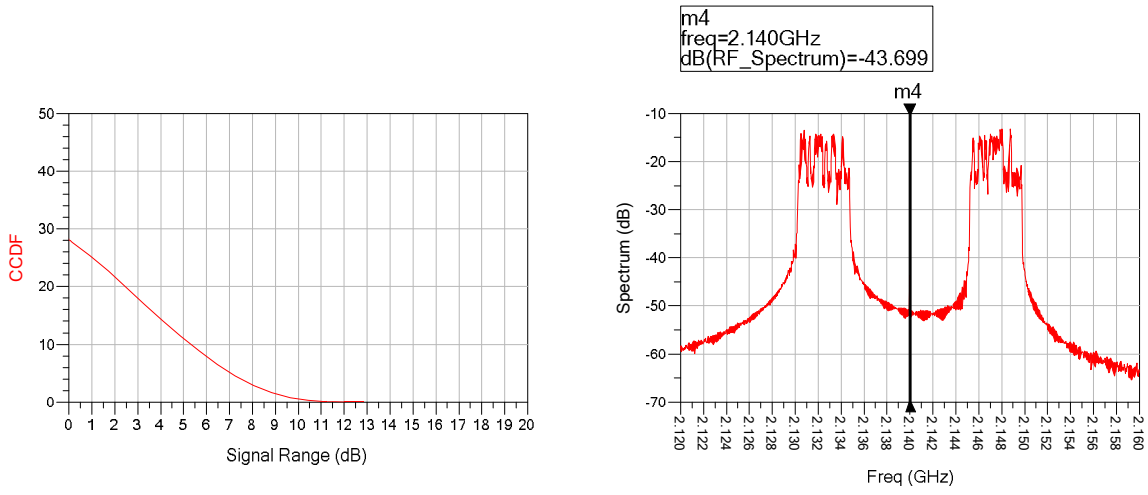

Figure 3.10: Signal CCDF and spectrum.

Figure 3.11 shows a part of the schematic used to simulate the ETPA. In this Figure the **VtDataset** source reads the dataset from the LTE signal simulation. This source allows

for increasing or decreasing the signal's amplitude through the use of the **Gain** parameter. Furthermore, it allows the designer to set the signal carrier frequency to whatever needed through changing **Freq** parameter. In this work, the **Gain** parameter was set to 1 whereas the **Freq** parameter was set to 2.14 GHz. "Circuit Envelope" simulation was used in ETPA design since it is very powerful in dealing with modulated signals along with analog circuits.

For the detection of the modulated signal envelope, the **IQ_DemodTuned** component was used to detect the real and imaginary parts of the input modulated signal as can be seen in Figure 3.11.

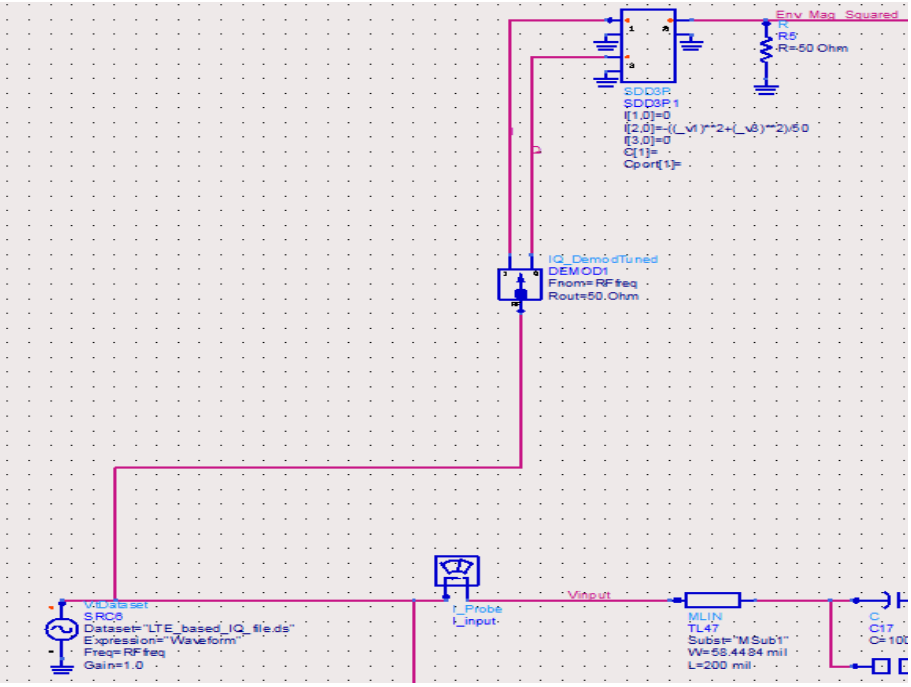

Figure 3.11: Part of the ETPA envelope path.

The voltage at node **Env_Mag_Squared** is equal to I^2+Q^2, where I is the real part of the input signal envelope and Q is its imaginary part. This computation was carried out

by the Symbolically-Defined Device (SDD) which generates a current into its port 2 given by

$$I_2 = \frac{-(v_1^2 + v_3^2)}{50} \tag{3.3}$$

The negative sign indicates positive current flowing out of port 2. Whereas v_1 is the voltage at port 1 and v_3 is the voltage at port 3 of the same component. This current flows into the 50 Ohm resistor, resulting in voltage **Env_Mag_Squared** being equal to $I^2 + Q^2$. With the magnitude of the input signal envelope in hand, the input signal power was calculated and then the drain bias was generated. As shown in Figure 3.12, The **Detected_Pin_dBm** equation represents available source power in dBm corresponding to the input signal samples. This input power was passed into the **Vdrain_vs_Pin_dBm.mdf** file, and the corresponding drain bias voltage was read and set equal to the **Vdrain** voltage with help of the Data Access Component (DAC).

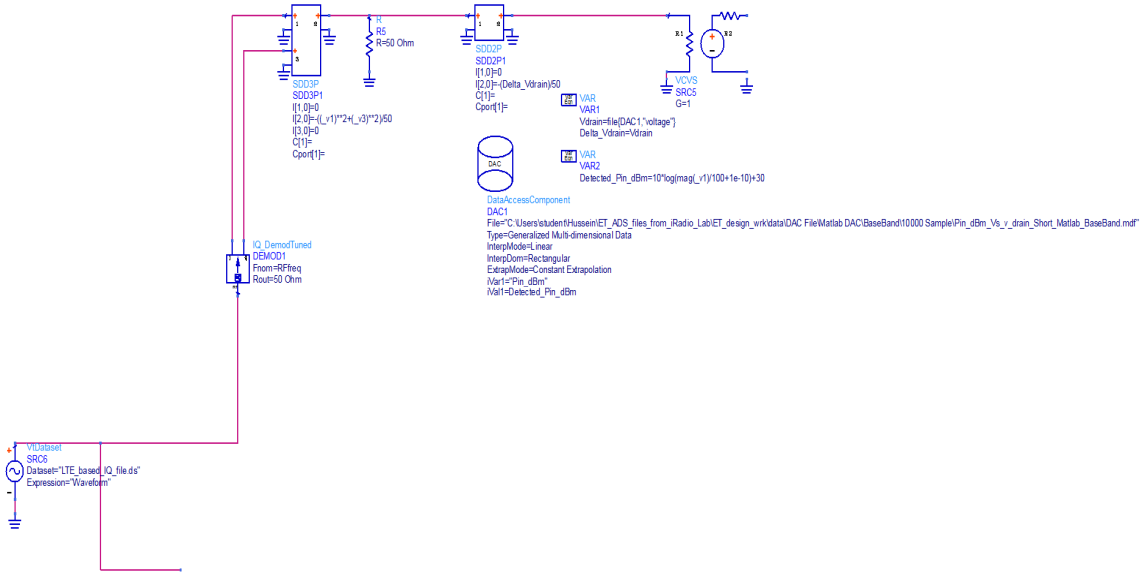

Figure 3.12: ETPA envelope path.

This **mdf** file is generated using a shaping function equation such as Nujira N6 and Nujira-Wilson. The sweeping range of the drain bias voltage was set from 10 to 30 volts as in the previous section. Figure 3.13 shows that the drain bias voltage closely follows the input signal power with 10 to 30 range when implementing Nujira N6 shaping function.

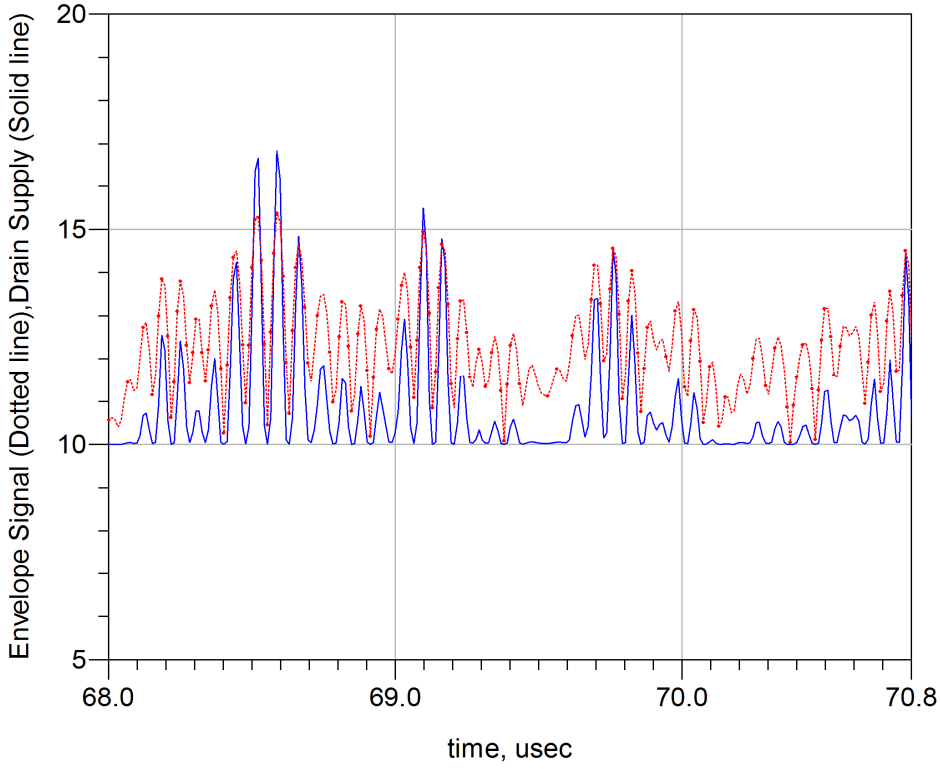

Figure 3.13: Input signal power and drain bias voltage generated using Nujira N6.

3.3.2 Applying the Envelope Tracking path to the Power Amplifier

Based on the optimum load found in the previous section, a PA was implemented. The conventional PA design steps were followed and basic input and output matching and biasing networks were constructed using Microstrip transmission lines, then the ET path designed in the previous subsection was applied to this efficiency optimized PA.

Moreover, a complete system level simulation circuit was built as illustrated in Figure 3.14 and the simulation was performed with the modulated LTE signal shown in Figure 3.10 to see how the ETPA behaves.

The main ETPA characteristics such as PAE, AM/AM, and AM/PM were calculated then reported in Figure 3.15. One important notice that could be drawn from this figure is that the PAE is maximized when the output power probability density function (PDF) is at its peak. In fact, the ET technique improves the PA efficiency compared with the fixed supply case as in Figure 3.8. However, AM/AM and AM/PM characterization show that this improvement is accompanied with more distortions indicated by the dispersion of these curves.

Due to the ETPA severe nonlinearities accurate behavioral models and digital predistorters should be developed to model and mitigate the memory effects observed in these types of power amplifiers.

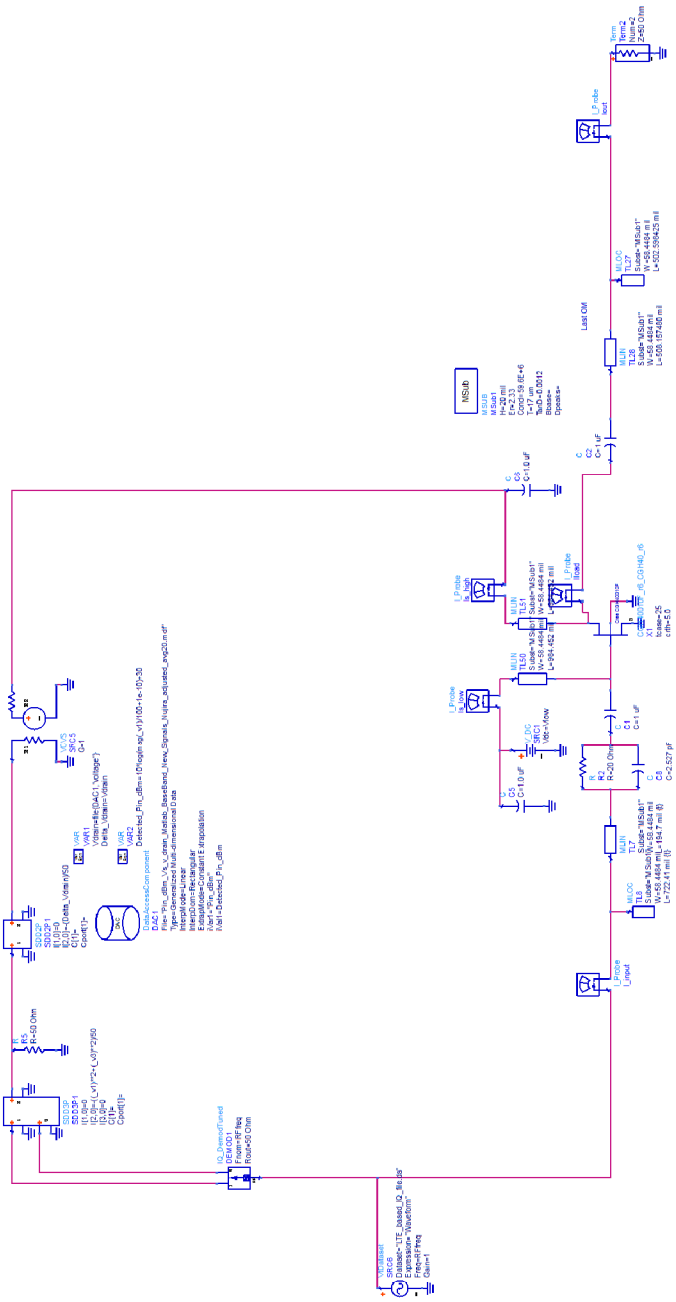

Figure 3.14: System level simulation of ETPA.

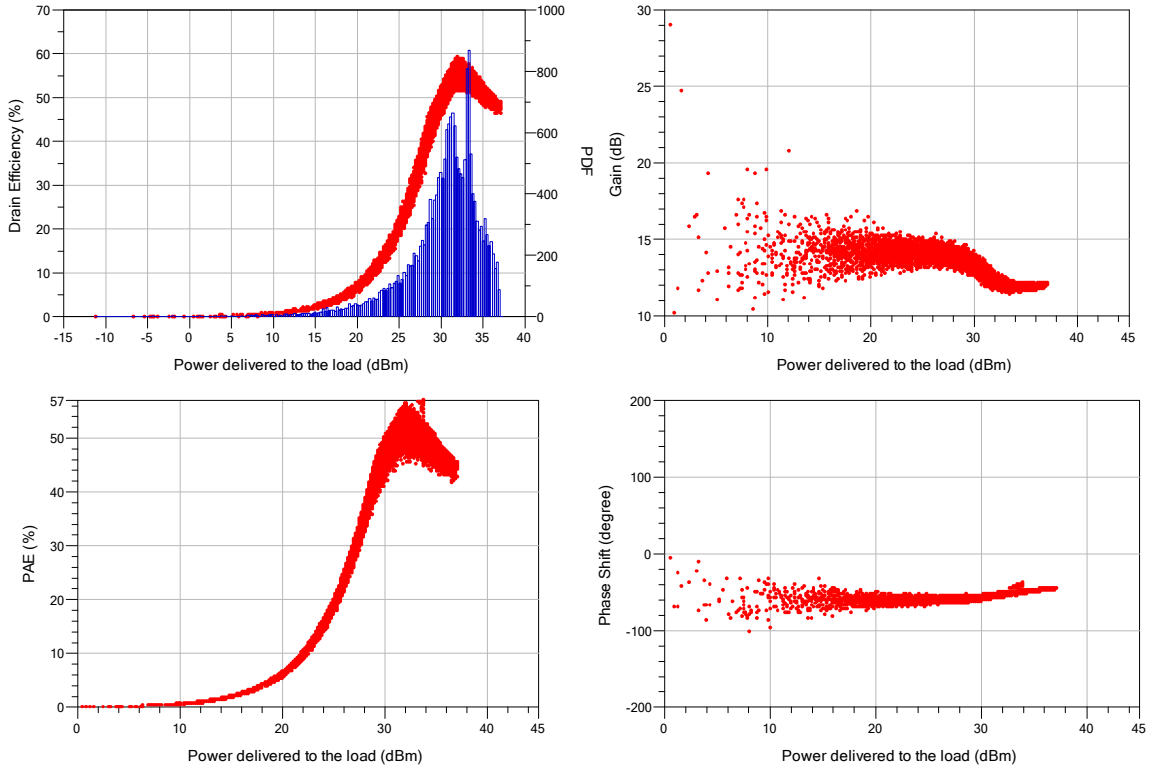

Figure 3.15: ETPA: drain efficiency, AM/AM, AM/PM, and PAE curves.

3.4 Summary and Discussion

In this chapter, a new method for selection of the output reflection coefficient was proposed. The method was developed for PAs which will be used in envelope tracking systems so it takes into account the nature of the signal and the shaping function to be applied. The method shows an increase of 3% in the average PAE over the conventional design method.

Furthermore, a complete ETPA system level simulation was implemented and used to better understand the ETPA behavior in order to come up with enhanced behavioral models.

CHAPTER 4

PROPOSED STRUCTURES FOR MODELING AND LINEARIZATION OF ENVELOPE TRACKING POWER AMPLIFIERS

This chapter investigates modeling and digital predistortion problems of envelope tracking power amplifiers. The first section discusses the various components in the measurement test bench that was used in ETPA measurements including device under test, measurements instruments, and signal characteristics, generation and control. The second section investigates the functions and structures proposed for modeling and digital predistorting the ETPA namely, the Volterra-series compressed sampling based behavioral model and the look-up table multi-input-single-output model (LUT-MISO). Then the proposed models are compared with state of the art models available in the literature and conclusions are drawn. The last section reports a summary of the main achievements that have been done in this chapter.

4.1 Experimental Setup

The measurement test bench shown in Figure 4.1 was used for testing the ET transmitter structure. The baseband signal generation and the control of the envelope modulator are done via a field programmable gate array (FGPA) board. The baseband signal is up-sampled by a factor of 2 then shifted to an intermediate frequency in order to avoid the digital to analog converter (DAC) AC-coupling effect. Then, the DAC output is passed through an anti-aliasing filter before sending it to the vector signal generator (VSG)

which up-converts the baseband signal and handles the power control of the RF signal. Finally, the RF signal is sent to the PA and the attenuated PA output is captured by a vector signal analyzer (VSA).

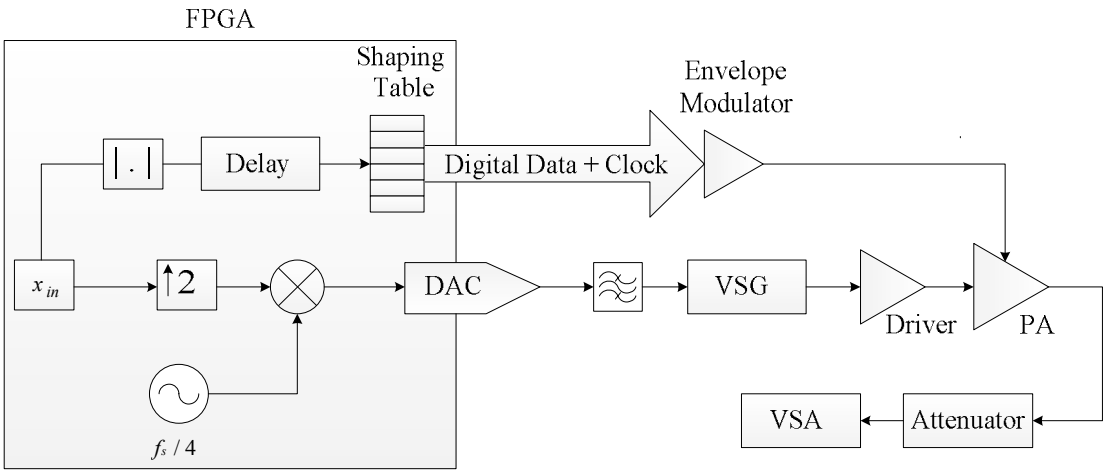

Figure 4.1: Block diagram of the envelope tracking power amplifier measurement setup.

Regarding the envelope modulator control, the magnitude of the complex baseband signal is properly delayed to correct for the propagation time difference between the application of the drain bias voltage and the input of the RF signal into the PA. Subsequently, this envelope signal is applied to the Nujira N6 shaping function that maps the digital input into an operating voltage used by the envelope modulator.

A Cree CGH40010 10-W transistor is used for the PA. The ET PA operates around 2.425 GHz and is optimized for efficiency at a quiescent drain voltage and current of 28 V and 200mA, respectively. The signal used in this thesis is a 4-carrier WCDMA signal centered at 2.425 GHz with a peak to average power ratio (PAPR) of 9.73 dB and a total bandwidth of 18 MHz. The signal is operated at a baseband sampling frequency of

122.88 MHz and the Nujira envelope modulator voltage swing is set between V_{min} = 10 V and V_{max}= 28 V.

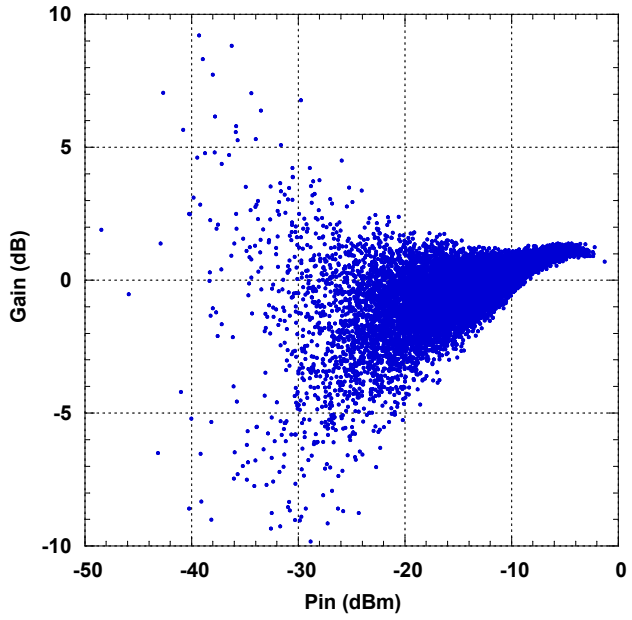

Figure 4.2: Measured AM/AM characteristic of the DUT.

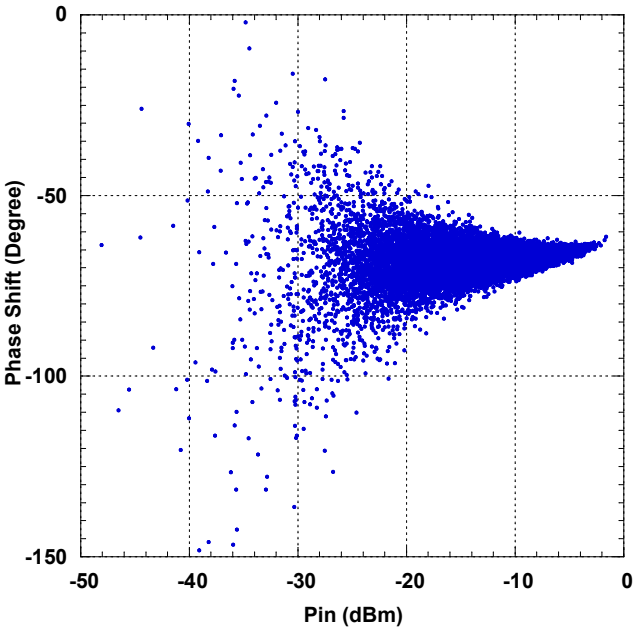

Figure 4.3: Measured AM/PM characteristic of the DUT.

The measured AM/AM and the AM/PM are shown in Figure 4.2 and Figure 4.3, respectively. The characteristics reported in these two figures clearly illustrate the highly nonlinear behavior of the device under test and its strong memory effects, which can be observed from the spread (or width) of the AM/AM and AM/PM curves.

4.2 Volterra Series with Compressed Sampling Behavioral Model

4.2.1 Volterra Series Model

The Volterra series model is the most comprehensive class of models used to describe the behavior of dynamic nonlinear systems. In this model, described below, all of the possible interactions between signal terms are taken into account, which explains the high accuracy of the model but also leads to a very large number of coefficients. To achieve a good compromise between the desirable performance of the model and implementation complexity, simplified variants have been proposed in the literature [49][50]. Among these variants, the simplified Volterra model in [49] was found to perform well. The expression for this model is described by the following equations:

$$y_{VS}(n) = y_A(n) + y_B(n) \tag{4.1}$$

$$y_A(n) = \sum_{n_1=0}^{N-1} a_1(n_1) x(n-n_1) + \sum_{n_1=0}^{N-1} \sum_{n_2=n_1-D}^{n_1} a_2(n_1,n_2) x(n-n_1) \left| x(n-n_2) \right| + \sum_{n_1=0}^{N-1} \sum_{n_2=n_1-D}^{n_1} \cdots \sum_{n_K=n_{K-1}-D}^{n_{K-1}} a_K(n_1,n_2,\cdots,n_K) x(n-n_1) \left| x(n-n_2) \right| \cdots \left| x(n-n_K) \right| \tag{4.2}$$

$$y_B(n) = \sum_{n_1=0}^{N-1} b_1(n_1) x(n-n_1)^* + \sum_{n_1=0}^{N-1} \sum_{n_2=n_1-D}^{n_1} b_2(n_1,n_2) x(n-n_1)^* \left|x(n-n_2)\right| + \sum_{n_1=1}^{N-1} \sum_{n_2=n_1-D}^{n_1} \cdots \sum_{n_K=n_{K-1}-D}^{n_{K-1}} b_K(n_1,n_2,\cdots,n_K) x(n-n_1)^* \left|x(n-n_2)\right| \cdots \left|x(n-n_K)\right| \tag{4.3}$$

where N is the nonlinearity order, $y_{VS}(n)$ is the model's output waveform, and $x(n)$ its input. D is the order of deviation, and a_k and b_k are the model coefficients. As demonstrated in [49], the practicality of this model can be greatly enhanced by using model-order reduction techniques such as the compressed sampling (CS) based method. This technique is used here to enhance the Volterra model performance when applied for the behavioral modeling of ET PA.

4.2.2 The Compressed Sampling (CS) Algorithm

Compressed sampling is a mathematical technique which attempts to reduce the complexity of a modeling problem through utilizing the redundancy and sparsity properties of the problem [51]. To define sparsity in the behavioral modeling context, the PA behavioral modeling is rewritten in the form of a linear problem as follows

$$\mathbf{y} = \mathbf{A}\,\mathbf{w} \tag{4.4}$$

where $\mathbf{y}$ is the vector containing all of the output samples as defined for the MP and Volterra models, $\mathbf{A}$ is the respective matrix defining the model (which is generated by collecting the various delayed and polynomial versions of input samples according to each respective model) and $\mathbf{w}$ is a vector containing the model coefficients (i.e. the set of $w_{l,k}$ for the MP model and the collection of a_k and b_k for the Volterra model).

In terms of this notation, the model coefficients vector $\mathbf{w}$ is considered 'sparse' if the majority of its entries are of zero or negligible value, which is the case for Volterra-based models. In mathematical terms, implementing CS is equivalent to trying to find an approximation of the vector $\mathbf{w}$ which contains the least number of terms. In [49], this technique was successfully implemented to significantly lower the number of coefficients used by the simplified Volterra model of equations (4.1)-(4.3), resulting in models which reduce by 80% the number of coefficients without performance degradation.

4.2.3 Behavioral Modeling using Volterra Series and Compressed Sampling

To evaluate the ability of the memory polynomial and the Volterra series models in predicting the output of the ET PA, the parameters of each model were varied and their performances in terms of normalized mean squared error recorded. In this work, the parameter-extraction was performed twice. Once using the well-known least squares (LS) method, and once using the compressed sampling technique. Figure 4.4 presents the best performance of each model when extracted with LS as a function of its number of coefficients. As expected, the Volterra series model outperforms the memory polynomial model at the expense of a larger model size.

The compressed sampling technique was then applied to reduce the sizes of the memory polynomial and Volterra series models. This allowed for substantial gain in terms of complexity without significant degradation of the models performances, as can be seen in Figure 4.5. In fact, the CS-reduced Volterra series model can lead to an NMSE better than -41dB with as low as 30 coefficients. This performance requires a Volterra series model with approximately 60 coefficients when CS is not applied, and cannot be reached by a memory polynomial model even by increasing the size up to 200 coefficients.

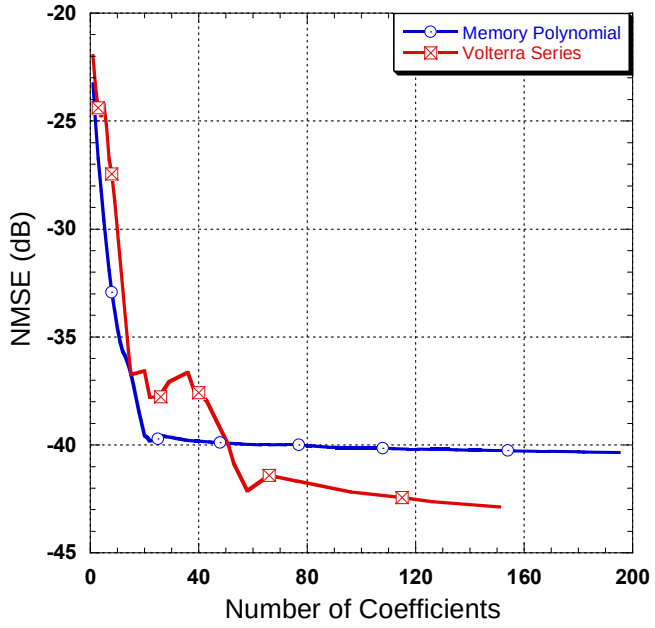

Figure 4.4: Performance of the Volterra series and MPM models extracted using the LS techniques.

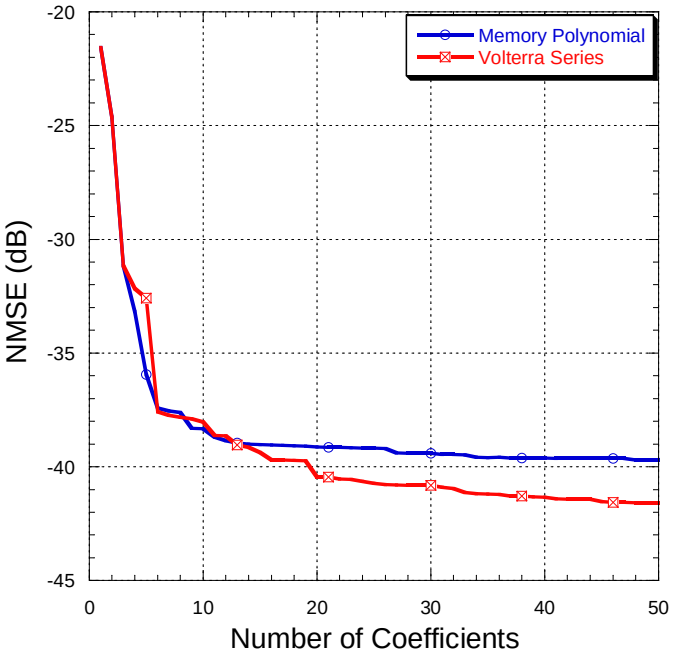

Figure 4.5: Performance of the Volterra series and MPM models after size reduction using the compressed sampling technique.

4.3 Look-Up Table Multi Input Memory Polynomial (LUT-MISO) Model

This model is composed of two boxes; where a memoryless nonlinear function is followed by a two-input memory polynomial model. Figure 4.6 shows a block diagram of this model coefficients identification process.

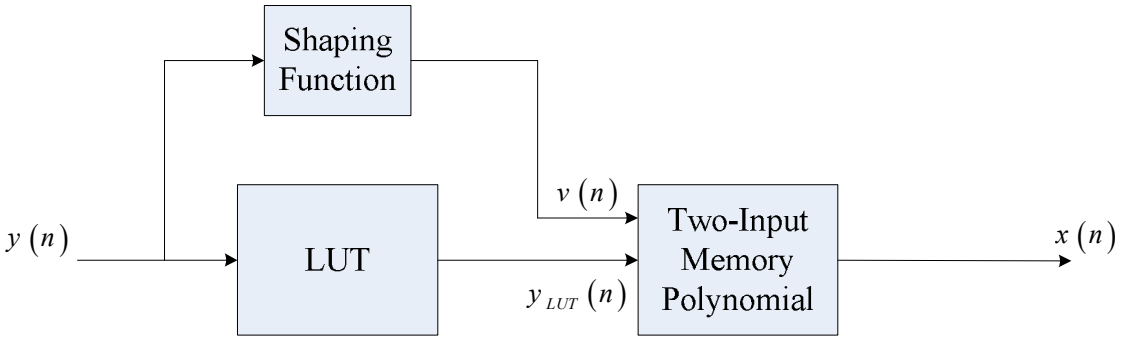

Figure 4.6: Coefficients identification block diagram.

Here, $y(n)$ is the complex PA output divided by the small signal gain, drain bias $v(n)$ is the output of the shaping function, $y_{LUT}(n)$ is the LUT output, and $x(n)$ is the PA complex input signal. Thus the DPD equation could be written as

$$x(n)=\sum_{j=0}^{M}\sum_{q=0}^{Q}\sum_{i=0}^{N}\sum_{p=0}^{P}a_{piqj}\left(v(n-j)\right)^{q}\, y_{LUT}(n-i)\left|y_{LUT}(n-i)\right|^{p} \tag{4.5}$$

where a_{piqj} are the model coefficients, P is the input nonlinearity order, N is the input taps, Q is the drain bias nonlinearity order, and M is the drain bias taps.

The proposed model is compared with two other models. The first one is the conventional two-box model in which a memoryless nonlinear function is followed by a single-input-single-output model as in equation (2.22). The other model is the dual-input-single-output

model proposed in [46]. The in-band performances of the digital predistorters extracted using these three models were compared in terms of NMSE against the models' number of coefficients and the results are shown in Figure 4.7 and Figure 4.8 for Nujira N6 and Nujira-Wilson shaping functions, respectively. As it can be seen, the dual-input models have better NMSE values that can go as low as -44 dB with 200 coefficients compared to only -40 dB obtained by the single-input model when drain bias is modulated by Nujira shaping function. The same dual-input model's NMSE performance could be noticed for Nujira-Wilson shaping function. However, -41 dB NMSE could be achieved using the single-input-single-output model. For number of coefficients less than 50, the proposed model is always better than model in [46] with NMSE difference of approximately 1 dB.

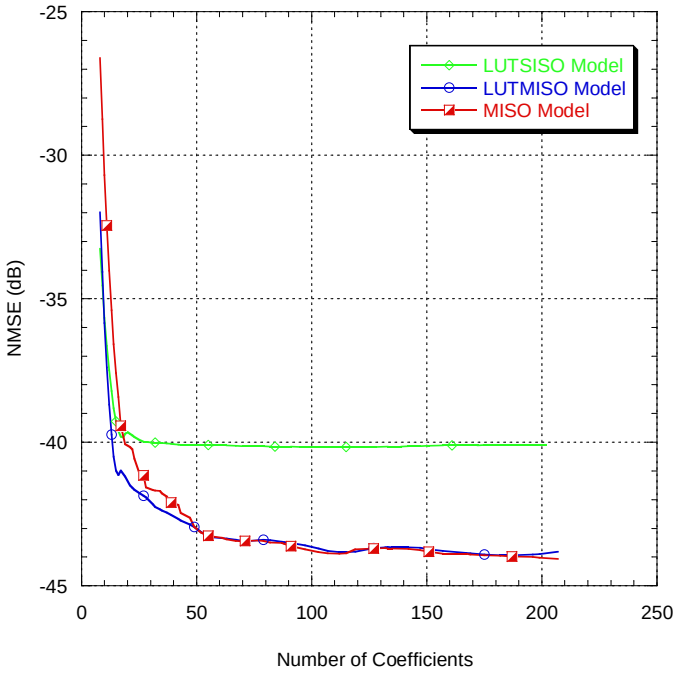

Figure 4.7: Performance of LUT-SISO, MISO, and LUT-MISO models extracted using the LS techniques for Nujira N6 shaping function case.

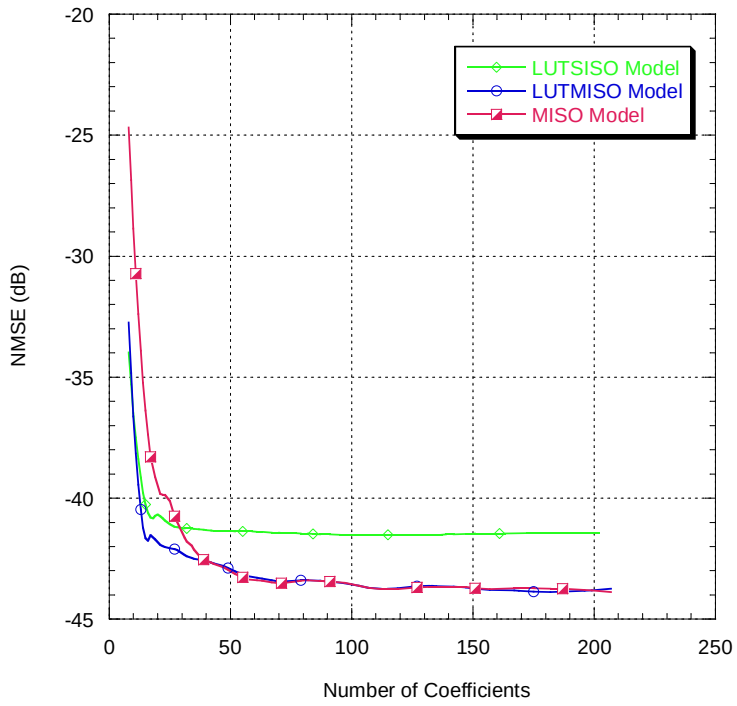

Figure 4.8: Performance of LUT-SISO, MISO, and LUT-MISO models extracted using the LS techniques for Nujira-Wilson shaping function case.

Figure 4.7 and Figure 4.8 give indication about the in-band performance of the three models. However, they do not describe the out-of-band digital predistorter performance. To do so, the three models predistorted signals were formed and applied to the ETPA and their corresponding output signals spectra were captured and compared to the original ETPA output spectrum (No DPD) as in Figure 4.9 and Figure 4.10 for Nujira N6 and Nujira-Wilson shaping functions, respectively. Figure 4.9, LUT-SISO, MISO, and LUT-MISO models spectra are compared with number of coefficients of 42 for each model. For LUT-SISO, the input nonlinearity order $(P)=6$, the input memory depth $(N)=6$, and $LUT\ size=7$. However, for MISO model, the model parameters are: $P=3$, $N=7$, $Q=2$, and $M=1$. Finally, the LUT-MISO model parameters are: $P=3$,

$N = 6$, $Q = 2$, $M = 1$, and $LUT\ size = 7$. In Figure 4.10, these three models are compared with a number of coefficients equals to approximately 26. Where $P = 5$, $N = 4$ and $LUT\ size = 7$ for LUT-SISO whereas $P = 2$, $N = 2$, $Q = 2$, and $M = 1$ for MISO model and finally, $P = 2$, $N = 5$, $Q = 2$, $M = 1$, and $LUT\ size = 7$ for LUT-MISO model. The lower and upper band ACPR values were calculated and they are compared in Table 4.1.

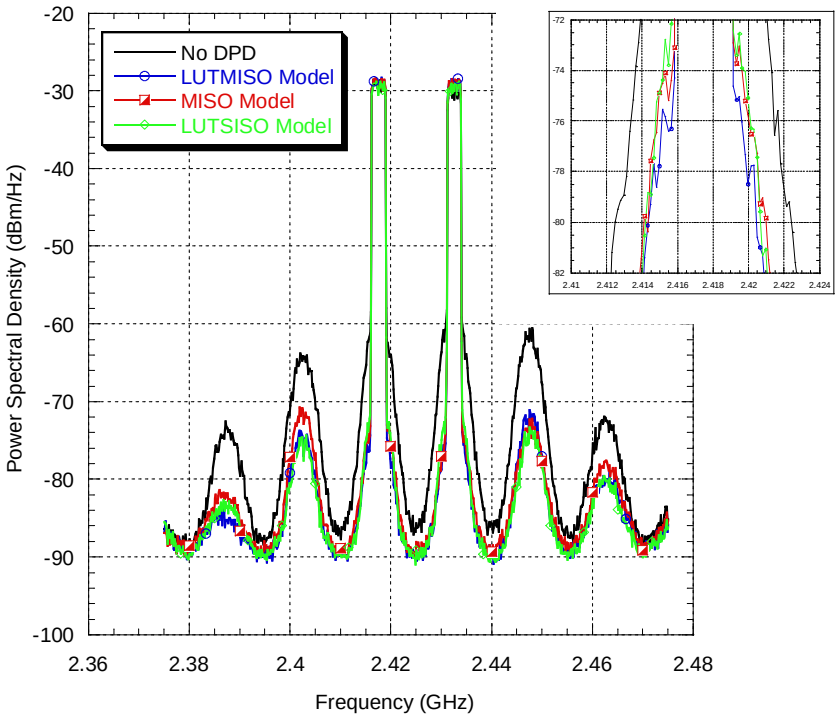

Figure 4.9: Linearized spectra for different models with Nujira N6 shaping function.

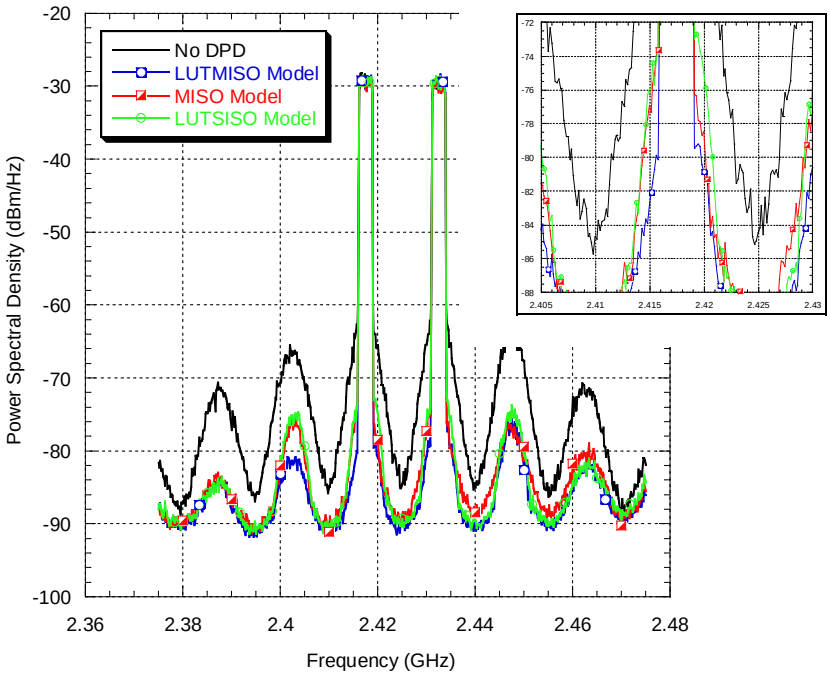

Figure 4.10: Linearized spectra for different models with Nujira-Wilson shaping function.

As it can be seen from the signal spectra and Table 4.1, the proposed model has the best linearization performance not only in terms of in-band performance but also in terms of the out-of-band performance.

Table 4.1: ACPR Performance Results Comparison

Model	**Number of Coefficients**		**ACPR (dBc)**	
	Nujira	Wilson	Nujira	Wilson
No DPD	-	-	-35.25/-41.11	-36.37/-41.42
LUT-SISO	42	25	-42.85/-50.98	-43.59/-50.96
MISO	42	24	-43.47/-50.94	-43.68/-53.50
LUT-MISO	42	26	-44.30/-52.86	-45.32/-55.15

4.4 Summary and Discussions

In this chapter, the targeted ETPA has been successfully modeled and linearized. Measurements results show that the Volterra-series with compressed sampling model can accurately predict the highly nonlinear behavior and the strong dynamic distortions of ETPAs with relatively low complexity when the CS technique is employed. In fact, the CS-reduced Volterra series model can lead to an NMSE better than -41dB with as low as 30 coefficients.

Moreover, the LUT-MISO and MISO models are undoubtedly better than LUT-SISO in terms of in-band performance. Approximately, 2dB to 4dB NMSE difference with a model size of 50 is observed for Nujira-Wilson and Nujira N6 shaping functions, respectively, with LUT-MISO model 1 dB better than MISO model with model size less than 50 coefficients. However, regarding the out-of-band performance, the LUT-MISO outperforms the MISO model as can be seen in the measured ACPR values in Table 4.1.

CHAPTER 5

SUMMARY AND CONCLUSIONS

5.1 Summary

This thesis thoroughly investigated the design, modeling, and linearization of envelope tracking power amplifiers. Significant contributions were made in regards to these three problems. The research done in this thesis is summarized as follows.

- A novel method was proposed for selecting the load reflection coefficient so that the average efficiency is maximized when the PA operates in ET configuration.
- An ET path was constructed, attached to the implemented PA, and then a complete ETPA system level simulation was fully implemented. The ETPA system level simulation was carefully tested with LTE signals and various shaping functions, and it demonstrated robust operation.
- A Single-input-single-output Volterra Series based behavioral model was used to mimic ETPA nonlinearities. However, the model suffered from high complexity. Thus, CS technique was implemented as extra task to solve this problem. The developed model was compared with the traditional memory polynomial model and their NMSE performances were calculated as a function of complexity (number of coefficients).
- Two-box dual-input-single-output memory polynomial model was developed and used as a digital predistorter for linearizing the efficiency-optimized ETPA. The

developed model was also compared with the conventional two-box single-input-single-output memory polynomial model as well as the single-box dual-input-single-output memory polynomial in terms of the in-band performance as well as the adjacent channel power ratio.

5.2 Conclusions

In conclusion there are three main ETPA problems which were identified, discussed, and then solved in this thesis.

- It has been shown that, based on the newly developed load reflection coefficient selection approach, the average PAE of ET PAs could be increased by 3% to 5% with no need to use any additional hardware processing.
- In this thesis, the nonlinearities of an efficiency-optimized ET PA were modeled using a Volterra series-based behavioral model. The complexity problem of the Volterra series is solved using the CS technique. Measurements results show that this model can accurately predict the highly nonlinear behavior and the strong dynamic distortions of ET PAs with relatively low complexity when the CS technique is employed.
- Two-box dual-input-single-output memory polynomial digital predistorter has superior in and out of band performances compared with single-box single-input-single output and conventional memory polynomial models.

5.3 Future Work

Specific suggestions for future work include

- Investigating envelope bandwidth reduction algorithms in order to relax the envelope amplifier designing requirements.
- Applying the proposed models to other dual-input architectures such dual-input Doherty and dynamic load modulation power amplifiers.

References

[1] ETSI, "Environmental engineering measurement method for energy efficiency of wireless access network equipment," 2011-10.

[2] S. C. Cripps, *RF power amplifiers for wireless communicataions*, 2nd ed., Norwood, MA: Artech House, 2006, pp. 42–46,

[3] B. Kim, I. Kim, and J. Moon, "Advance doherty architecture," *IEEE Microw. Mag.*, vol. 11, no. 5, pp. 72-86, Aug. 2010.

[4] F. Wang, A. Ojo, D. Kimball, P. Asbeck, and L. Larson, "Envelope tracking power amplifier with pre-distortion linearization for WLAN 802.11g," in *IEEE MTT-S Int. Microw. Symp. Dig.*, Jun. 2004, pp. 1543 – 1546.

[5] http://www.rf-design-tips.com/wp-content/uploads/2012/02/ADS-Envelope%20Tracking.pdf

[6] P. Draxler, J. J. Yan, D. F. Kimball, and P. M. Asbeck, "Digital predistortion for envelope tracking power amplifiers," in *Wirel. and Microw. Tech. Conference*, Cacoa Beach, FL, USA, Apr. 2012, pp. 1–7

[7] Y. Y. Woo, Y. Yang, J. Yi, J. Nam, J. H. Cha, and B. Kim, "Feedforward amplifier for WCDMA base stations with a new adaptive control method," in *IEEE MTT-S Int. Microw. Symp. Dig.*, Seattle, WA, USA, Jun. 2002, pp. 769–772.

[8] Y. Kim, Y. Yang, S. Kang, and B. Kim, "Linearization of 1.85 GHz amplifier using feedback predistortion loop," in *IEEE MTT-S Int. Microw. Symp. Dig.*, Baltimore, MD, USA, Jun. 1998, pp. 1675–1678.

[9] H. H. Chen, C.-H. Lin, P.-C. Huang, and J.-T. Chen, "Joint polynomial and look-up-table predistortion power amplifier linearization," *IEEE Trans. Circuits Syst. II Express Briefs*, vol. 53, no. 8, pp. 612–616, Aug. 2006.

[10] T. J. Brazil, "An adaptive Volterra predistorter for the linearization of RF high power amplifiers," in *IEEE MTT-S Int. Microw. Symp. Dig.*, Seattle, WA, USA, Jun. 2002, pp. 461–464.

[11] N. Safari, T. Roste, P. Fedorenko, and J. S. Kenney, "An approximation of Volterra series using delay envelopes, applied to digital predistortion of RF power amplifiers with memory effects," *IEEE Microw. Wireless Compon. Lett.*, vol. 18, no. 2, pp. 115–117, Feb. 2008.

[12] J. Kim and K. Konstantinou, "Digital predistortion of wideband signals based on power amplifier model with memory," *Electron. Lett.*, vol. 37, no. 23, p. 1417-1418, Nov. 2001.

[13] F. M. Ghannouchi and O. Hammi, "Behavioral modeling and predistortion," *IEEE Microw. Mag.*, vol. 10, no. 7, pp. 52–64, Dec. 2009.

[14] J. K. Cavers, "Amplifier linearization using a digital predistorter with fast adaptation and low memory requirements," *IEEE Trans. Veh. Technol.*, vol. 39, no. 4, pp. 374–382, Nov. 1990.

[15] P. L. Gilabert, G. Montoro, and E. Bertran, "On the Wiener and Hammerstein models for power amplifier predistortion," in *Asia-Pacific Microwave Conference Proceedings*, Dec. 2005, pp. 1–4.

[16] L. Taijun, S. Boumaiza, and F. M. Ghannouchi, "Deembedding static nonlinearities and accurately identifying and modeling memory effects in wide-band RF transmitters," *IEEE Trans. Microw. Theory Tech.*, vol. 53, no. 11, pp. 3578–3587, Nov. 2005.

[17] L. Taijun, S. Boumaiza, and F. M. Ghannouchi, "Augmented hammerstein predistorter for linearization of broad-band wireless transmitters," *IEEE Trans. Microw. Theory Tech.*, vol. 54, no. 4, pp. 1340–1349, Jun. 2006.

[18] O. Hammi, F. M. Ghannouchi, and B. Vassilakis, "A compact envelope-memory polynomial for RF transmitters modeling with application to baseband and RF-digital predistortion," *IEEE Microw. Wirel. Components Lett.*, vol. 18, no. 5, pp. 359–361, May 2008.

[19] O. Hammi, M. Younes, and F. M. Ghannouchi, "Metrics and methods for benchmarking of RF transmitter behavioral models with application to the development of a hybrid memory polynomial model," *IEEE Trans. Broadcast.*, vol. 56, no. 3, pp. 350–357, Sep. 2010.

[20] D. R. Morgan, Z. Ma, J. Kim, M. G. Zierdt, and J. Pastalan, "A generalized memory polynomial model for digital predistortion of RF power amplifiers," *IEEE Trans. Signal Process.*, vol. 54, no. 10, pp. 3852–3860, Oct. 2006.

[21] O. Hammi, A. M. Kedir, and F. M. Ghannouchi, "Nonuniform memory polynomial behavioral model for wireless transmitters and power amplifiers," in *Asia Pacific Microw. Conference Proceedings*, Kaohsiung, Taiwan, Dec. 2012, pp. 836–838.

[22] O. Hammi and F. M. Ghannouchi, "Twin nonlinear two-box models for power amplifiers and transmitters exhibiting memory effects with application to digital

predistortion," *IEEE Microw. Wireless Compon. Lett.*, vol. 19, no. 8, pp. 530–532, Aug. 2009.

[23] M. Younes, O. Hammi, A. Kwan, and F. M. Ghannouchi, "An accurate complexity-reduced 'PLUME' model for behavioral modeling and digital predistortion of rf power amplifiers," *IEEE Trans. Ind. Electron.*, vol. 58, no. 4, pp. 1397–1405, Apr. 2011.

[24] O. Hammi, M. S. Sharawi, and F. M. Ghannouchi, "Generalized twin-nonlinear two-box digital predistorter for GaN based LTE doherty power amplifiers with strong memory effects," in *IEEE Int. Wireless Symp.*, Beijing, China, Apr. 2013, pp. 1–4.

[25] A. Zhu and T. J. Brazil, "An overview of volterra series based behavioral modeling of RF/microwave power amplifiers," in *IEEE Annual Wireless and Microw. Technol. Conference*, Clearwater Beach, FL, USA, Dec. 2006, pp. 1–5.

[26] D. Mirri, G. Luculano, F. Filicori, G. Pasini, G. Vannini, and G. P. Gabriella, "A modified Volterra series approach for nonlinear dynamic systems modeling," *IEEE Trans. Circuits Syst. I Fundam. Theory Appl.*, vol. 49, no. 8, pp. 1118–1128, Aug. 2002.

[27] A. Zhu, J. Dooley, and T. Brazil, "Simplified Volterra series based behavioral modeling of RF power amplifiers using deviation-reduction," in *IEEE MTT-S Int. Microw. Symp. Dig.*, San Francisco, CA, USA, Jun. 2006, pp. 1113–1116.

[28] J. Staudinger, "DDR Volterra series behavioral model with fading memory and dynamics for high power infrastructure amplifiers," in *IEEE Topical Conference on Power Amplifiers for Wireless and Radio Applications*, Phoenix, AZ, USA, Jan. 2011, pp. 61–64.

[29] J. Jeong, D. F. Kimball, M. Kwak, C. Hsia, P. Draxler, and P. M. Asbeck, "Wideband envelope tracking power amplifiers with reduced bandwidth power supply waveforms and adaptive digital predistortion techniques," *IEEE Trans. Microw. Theory Tech.*, vol. 57, no. 12, pp.3307–3314, Dec. 2009.

[30] D. Rudolph, "Kahn EER technique with single-carrier digital modulations," *IEEE Trans. Microw. Theory Tech.*, vol. 51, no. 2, pp. 548–552,Feb. 2003.

[31] G. Montoro, P.L. Gilabert, E. Bertran and J. Berenguer. "A method for real time generation of slew-rate limited envelopes in envelope tracking transmitters," *IEEE Int. Microw. Series on RF Front-ends for Soft. Defined and Cognitive Radio Solutions*, Aveiro, Portugal, Feb. 2010, pp. 1-4.

[32] J. Jeong, D. F. Kimball, M. Kwak, C. Hsia, P. Draxler, and P. M. Asbeck, "Wideband envelope tracking power amplifiers with reduced bandwidth power

supply waveform and adaptive digital predistortion techniques," *IEEE Trans. Microw. Theory Tech.*, vol. 57, no. 12, pp. 3307–3314, Dec. 2009.

[33] P.P. Vizarreta, G. Montoro, and P.L. Gilabert, "Hybrid envelope amplifier for envelope tracking power amplifier transmitters", in *European Microwave Conf.*, Amsterdam, Holland, Nov. 2012, pp. 128-131.

[34] A. Zhu, P. J. Draxler, C. Hsia, T. Brazil, D. F. Kimball, and P. M. Asbeck, "Digital predistortion for envelope-tracking power amplifiers using decomposed piecewise Volterra series," *IEEE Trans. Microw. Theory Tech.*, vol. 56, no. 10, pp. 2237–2247, Oct. 2008.

[35] A.Hekkala, A. Kotelba, M. Lasanen, P. Järvensivu, and A. Mämmelä, "Novel digital compensation approaches for envelope tracking amplifiers," *Wireless. Pers. Commun.*, to be published.

[36] I. Kim, Y. Y. Woo, J. Kim, J. Moon, J. Kim, and B. Kim, "High-efficiency hybrid EER transmitter using optimized power amplifier," *IEEE Trans. Microw. Theory Tech.*, vol. 56, no. 11, pp. 2582–2593, Nov.2008.

[37] I. Kim, J. Kim, J. Moon, and B. Kim, "Optimized envelope shaping for hybrid EER transmitter of mobile Wimax-optimized ET operation," *IEEE Trans. Microw. Wireless Compon. Lett.*, vol. 19, no. 5, pp. 335–337, May 2009.

[38] A. Zhu, J. C. Pedro, and T. J. Brazil, "Dynamic deviation reduction-based Volterra behavioral modeling of RF power amplifiers," *IEEE Trans. Microw. Theory Tech.*, vol. 54, no. 12, pp. 4323–4332, Dec. 2006.

[39] H. Harju, T. Rautio, S. Hietakangas, and T. Rahkonen, "Envelope tracking power amplifier with static predistortion linearization," in *European Conf. Circuit Theory and Design*, Seville, Spain, Aug. 2007, pp. 388-391.

[40] H. Cao, H. M. Nemati, A. S. Tehrani, T. Eriksson, and C. Fager. "Digital predistortion for high efficiency power amplifier architectures using a dual-input modeling approach," *IEEE Trans. Microw. Theory Tech.*,vol. 60, no. 2, pp. 361-369, Feb. 2012.

[41] P. Gilabert, G. Montoro, and P. Vizarreta, "Slew-rate and efficiency trade-off in slow envelope tracking power amplifiers," in *The 7th German Microwave Conference*, Ilmenau, Germany, Mar. 2012, pp. 1–4.

[42] H. Cao, H. M. Nemati, A. S. Tehrani, T. Eriksson, and J. Grahn, "Linearization of efficiency-optimized dynamic load modulation transmitter architectures," *IEEE Trans. Microw. Theory Tech.*, vol. 58, no. 4, pp. 873–881, Apr. 2010.

[43] H. M. Nemati, H. Cao, B. Almgren, T. Eriksson, and C. Fager, "Design of highly efficient load modulation transmitter for wideband cellular applications," *IEEE Trans. Microw. Theory Tech.*, vol. 58, no. 11, pp. 2820–2828, Nov. 2010.

[44] M. López, Gabriel, G. Pinal, P. Lluís, V. Paz, and P. Pablo, "Incremental behavioral modeling of envelope-dependent nonlinear distortion in dynamic supply power amplifiers, " *E-prints UPC -Universitat Politecnica de Catalunya*

[45] G. Montoro, P. L. Gilabert, J. Berenguer, and E. Bertran, "Digital predistortion of envelope tracking amplifiers driven by slew-rate limited envelopes," in *IEEE MTT-S Int. Microw. Symp. Dig.*, Baltimore, MD, USA, Jun. 2011, pp. 1–4.

[46] G. Montoro and P. L. Gilabert, "Look-up table implementation of a slow envelope dependent digital predistorter for envelope tracking power amplifiers," *IEEE Microw. Wireless. Compon. Lett.*, vol. 22, no. 2, pp. 97–99, Feb. 2012.

[47] S.A. Cripps, "A theory for the prediction of GaAs FET load-pull power contours," in *IEEE MTT-S Int. Microw. Symp. Dig.*, Boston, MA, USA, May 1983, pp. 221-223.

[48] A. Cidronali, G. Manes, N. Giovannelli, T. Vlasits, and R. Hernaman, "Efficiency and linearity enhancements with envelope shaping control in dual-band envelope tracking GaAs PA," in *European Microw. Integrated Circuit Conf.*, Manchester, UK, Oct. 2011, pp. 308-311.

[49] A. Abdelhafiz, A. Kwan, O. Hammi, and F. M. Ghannouchi, "Digital predistortion of LTE-A power amplifiers using compressed-sampling-based unstructured pruning of Volterra series," *IEEE Trans. Microw. Theory Tech.*, vol. 62, no. 11, pp.2583-2593, Nov. 2014.

[50] A. Zhu and T. J. Brazil, "Behavioral modeling of RF power amplifiers based on pruned Volterra series," *IEEE Microw. Wireless Compon. Lett.*, vol. 14, no. 12, pp. 563-565, Dec. 2004.

[51] D. L. Donoho, "Compressed sensing," *IEEE Trans. Inf. Theory,* vol. 52, no. 4, pp. 1289-1306, Apr. 2006.

Vitae

Name	: Mohamed Osman Hussein Khalifa
Nationality	: Sudanese
Date of Birth	: 4/20/1989
Email	: g201202900@kfupm.edu.sa, mohkma@gmail.com
Address	: Hno 186, Mamoora, Khartoum, Sudan 11111
Academic Background	: MS in Electrical Engineering (Major: Electromagnetics) KFUPM, Dhahran 2015 BSc. in Electrical and Electronic Engineering, Khartoum University 2010

Publications and Patents

M.O. H. Khalifa, A.H. Abdelhafiz, and A. Zerguine, "Sparse channel estimation using adaptive filtering and compressed sampling," in *International Conference on Computing, Electrical and Electronics Engineering (ICCEEE),* Khartoum, Sudan, Aug. 2013 pp.144,147 (PUBLISHED).

M. O. H. Khalifa, Abubaker Abdelhafiz, Andrew Kwan, Fadhel M. Ghannouchi, and Oualid Hammi, "Behavioral Modeling of Envelope Tracking Power Amplifier using Volterra Series Model and Compressed Sampling" in *International Wireless Symposium (IWS),* Shenzhen, China, Mar. 2015 (ACCEPTED).

M. O. H. Khalifa and Oualid Hammi, "Design of Envelope Tracking Power Amplifier for LTE Applications" (JOURNAL READY TO SUBMIT).

M. O. H. Khalifa, Andrew Kwan, Fadhel M. Ghannouchi, and Oualid Hammi, "Two-Box Dual-Input Digital Predistortion for Envelope Tracking Power Amplifiers" (JOURNAL READY TO SUBMIT).

M. O. H. Khalifa and Oualid Hammi, "Design of Envelope Tracking Power Amplifier for LTE Applications" (PATENT IN PROGRESS).

M. O. H. Khalifa, Andrew Kwan, Fadhel M. Ghannouchi, and Oualid Hammi, "Two-Box Dual-Input Digital Predistortion for Envelope Tracking Power Amplifiers" (PATENT IN PROGRESS).